JOURNAL OF MATERIALS SCIENCE 28 (1993) 2557–2576

Review
Solid-solution hardening

M. Z. BUTT
Centre for Advanced Studies in Physics, PO Box 1750, Government College, Lahore, 54000, Pakistan

P. FELTHAM
Brunel University, Uxbridge, Middlesex, London, UB8 3PH UK

Recent advances in the understanding of solid-solution hardening (SSH) of crystalline materials, as well as some basic early papers are briefly reviewed. This survey shows that models of SSH based on the concept of a frictional drag on dislocations migrating through fields of point-like obstacles, whether randomly dispersed or clustered, do not encompass the principal features of SSH, e.g. the temperature dependence of the yield stress, the stress and temperature dependences of the activation volume, and the phenomenon of stress equivalence. However, a model based on the nucleation of slip, involving the breakaway of dislocation segments from several pinning points, formulated in closed form, is shown to account satisfactorily for the principal observations.

1. Introduction

The increase of the flow stress of a metal due to the presence of dispersed foreign atoms is referred to as solid-solution hardening (SSH). Two trends can be observed in the evolution of modern theories of SSH. In the first, typified by the classical paper of Mott and Nabarro [1], mutually non-interacting dislocations move under the applied shear stress piecewise through random dispersions of localized, point-like, attractive and repulsive barriers (Fig. 1); the solute concentration, c, is assumed to be high enough to involve several solute atoms in the advance of a dislocation segment, i.e. the models are collective. Suzuki [2] referred to these models as the friction type. They differ from models of the breakaway type, exemplified, for instance, by that of Friedel [3], in which the low solute concentration facilitates breakaway from individual pinners. Types of both models, proposed in the period 1948–1978 [e.g. 1, 3–19] were critically reviewed by Butt and Feltham [20] in 1978. Since then a number of papers on new developments in this field have appeared [e.g. 21–70]; these, as well as some basic early papers, will be referred to in this review.

2. Migration of dislocations through random dispersions of solute atoms

2.1. The model of Mott and Nabarro

In their pioneering work on SSH published in 1948, Mott and Nabarro [1] considered that on replacing some atoms of the solvent matrix by solute atoms, either larger or smaller than those of the solvent, the resulting local stresses led to interaction of the solute atoms with dislocations; the latter were regarded as akin to elastic strings with limited flexibility. The non-uniform internal stress field was postulated to vary spatially about a zero mean value with typical amplitude τ_i and wavelength λ; the latter was taken as equal to $bc^{-1/3}$, the mean solute spacing in the volume of the crystal. The solute atoms were assumed to be so closely spaced that the internal stresses could not force dislocations, which due to their line tension were not flexible enough, to undulate with the wavelength of this stress field. Thus each dislocation rode through the stress-field piecewise (Fig. 1). Although, in view of the alternating signs of the internal stress, the average force on a dislocation would, in general, be close to zero, local deviations would permit line elements of the dislocation, each of length $L \gg \lambda$, to move almost independently of the neighbouring segments flanking it.

Further, it was assumed that a dislocation segment of length $L \gg \lambda$, moving forward as an independent unit, is composed of L/λ elements, on each of which the internal stress exerts a force of magnitude $\tau_i b\lambda$, but of random sign. The statistical resultant of these random forces acting on the length L is $\tau_i b\lambda(L/\lambda)^{1/2}$, and flow will occur when the applied force τbL, experienced by the dislocation due to the external stress τ, is balanced by the former, so that then

$$\tau = \tau_L = \tau_i(\lambda/L)^{1/2} \quad (1)$$

The dislocation is effectively flexible under the mean internal stress τ_L, if L is so large that the radius of curvature, ρ_L, of the dislocation is about equal to L, i.e. if

$$L = \rho_L = E/(\tau_L b) \quad (2)$$

where $E(=\frac{1}{2}Gb^2)$ is the line energy per unit length of dislocation, and G the shear modulus. The magnitude of τ_i at the dislocation is estimated from the local volume average of the shear stress due to a single

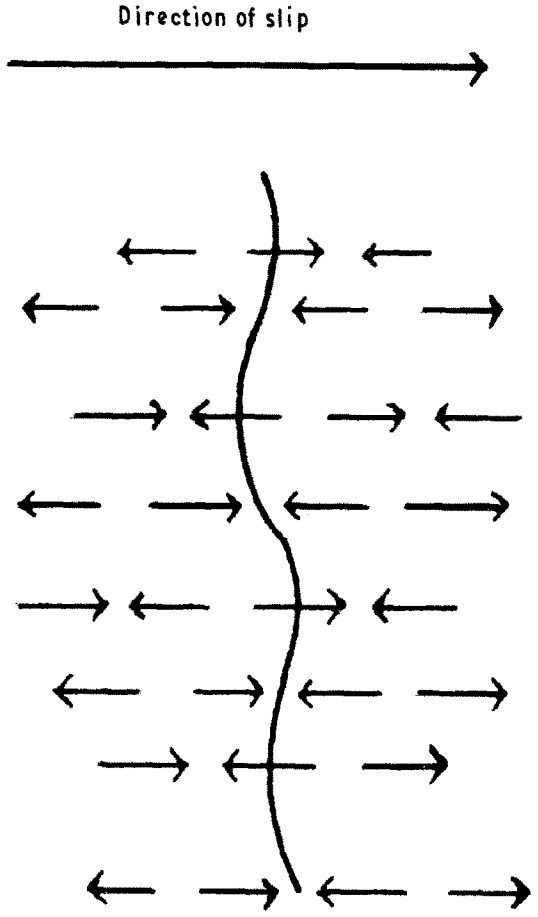

Figure 1 A wavy dislocation in the model of Mott and Nabarro. Arrows indicate the direction of the force which the internal stress exerts on the dislocation in the slip plane [1].

solute atom, and is given by

$$\tau_i = \frac{\int_b^\lambda (G\varepsilon_b b^3/r^3)4\pi r^2\,dr}{\int_b^\lambda 4\pi r^2\,dr} \simeq -G\varepsilon_b c(\ln c) \quad (3)$$

Where $\varepsilon_b = (1/b)(db/dc)$ is the size-misfit factor and c the solute concentration. The critical shear stress, obtained from Equations (1–3), is then found to be

$$\tau = G\varepsilon_b^2 c^{5/3}(\ln c)^2 \quad (4)$$

Although the theory is conceptually attractive, the result, i.e. the concentration dependence of the yield stress in shear implied by Equation 4, is not confirmed experimentally. In fact, one of the weaknesses of this theory is its applicability only to dislocations whose stress fields arise from volume strains, so that pure screw dislocations would not be interacting significantly with the solute, and would thus be able to move freely. Moreover, experiment shows (e.g. [4, 5]) that solute atoms with valencies differing markedly from those of the solvent have a greater hardening effect for a given size factor, ε_b, than those where valencies differ less from that of the solvent. Hence it would seem that in interpreting the hardness of alloys valency must also be taken into account, in addition to size misfit. However, as was pointed out by Fleischer [4], there remains no valency effect to be accounted for when allowance is made for the modulus mismatch, $\varepsilon_G = (1/G)(dG/dc)$, between solute and solvent atoms. Thermal activation of dislocation movement was not allowed for in the theory, which was thus confined to SSH at low temperatures.

2.2. The model of Labusch

Labusch [11] re-examined the alloy-hardening theory of Mott and Nabarro [1], and pointed out that, except in rather dilute solutions, solute atoms could not be assumed to be uniformly dispersed; groups of relatively closely spaced solute atoms would also exist, so that spatial fluctuations in obstacle density would occur in the crystal. Individual groups would act as single "effective" obstacles of strength exceeding that of isolated solute atoms, but less than the sum of their separate strengths, because, due to its line tension, a piece of dislocation would not in general be sufficiently flexible to make full contact with all the individual solute atoms comprising such a cluster. Nevertheless, for simplicity, the strength of an "effective" cluster obstacle was taken as being equal to the sum of the strength of individual solute atoms in the cluster. Its range of interaction, defined by $w = U_m/f_m$, where f_m is the maximum obstacle-dislocation interaction force and U_m the obstacle-to-dislocation interaction energy, was still taken to be of the same order as that ascribed to a single solute atom.

In contrast to the model of Mott and Nabarro [1], in which a dislocation has to ride over the internal stress field (Fig. 1) of dispersed "weak" obstacles, the dislocation was now assumed to interact strongly with the more localised "effective" obstacles, because the relatively intense stress field of clustered obstacles was assumed to lead to a closer adaptation of the dislocation to the cluster than to a similar number of individual, dispersed, solute atoms. Labusch's theory, essentially a development of that of Mott and Nabarro, is also of the collective type, for several solute atoms are again involved in the elementary breakaway process. Apart from the cluster concept, Labusch modified some "statistical" assumptions in the theory of Mott and Nabarro substituting more plausible ones; as a result he obtained the often observed e.g. [16, 30] $c^{2/3}$ relation for the concentration dependence of the flow stress in shear, replacing Equation 4 with

$$\tau = \frac{A}{b}(f_m^4 c^2 w/E)^{1/3} \quad (5)$$

The dependence of τ on temperature was not considered.

The constant, A, in Equation 5 depends on the form of the force–distance relation

$$f(y) = f_m(2y/w)/[1 + (y/w)^2]^2$$

assumed for the interaction between a dislocation and the obstacle located at a distance y from it. Here the maximum interaction force is $f_m = (Gb^2/120)\varepsilon_L$, the misfit parameter, ε_L, being given by a linear combination of the size and modulus factors: $\varepsilon_L = [(\varepsilon'_G)^2 + (\alpha\varepsilon_b)^2]^{1/2}$, where $\varepsilon'_G = \varepsilon_G/[1 + \frac{1}{2}|\varepsilon_G|]$, and the constant α is equal to ± 16 for edge dislocations.

The positive and negative values of α are appropriate for edge dislocations of corresponding signs.

2.3. Nabarro's theory

In a later paper Nabarro [18] briefly surveyed the subject of SSH, and then re-examined the basic features of the problem, i.e. the passage of a dislocation over a glide plane containing a concentration of randomly dispersed obstacles ($T \rightarrow 0$ K). These were represented by potential wells of a given width $2w$ (Fig. 2), each obstacle exerting an attractive force of maximum value f_m on the dislocation. For a solid solution sufficiently dilute to enable arcs of dislocations to break away from isolated pinning points individually, i.e. in the "Friedel limit" in which, according to Arsenault and Cadman [71], the solute content is less than 100–200 p.p.m., he obtained for the critical resolved shear stress (CRSS), τ, the relation

$$\tau = \frac{1}{b}(f_m^2 c/2^{5/2} E)^{1/2} \quad (6)$$

However, at relatively high concentrations the solute atoms will be rather closely spaced along a dislocation, and the breakaway-and-repinning process will involve a segment of dislocation containing many obstacles. For that case, he derived

$$\tau = \frac{1}{2b}(f_m^4 c^2 w/E)^{1/3} \quad (7)$$

Nabarro's model [18] may be regarded as basically a development of Labusch's [11] which, in turn, is similar in essence to the classical model of the passage of a dislocation through a random dispersion of obstacles advanced by Mott and Nabarro [1], discussed earlier. However, as in that paper [1], Nabarro [18] does not consider clustering, as envisaged by Labusch [11], as an essential feature or as a prerequisite of SSH. In its functional form Equation 7 agrees with Labusch's (Equation 5); the $c^{2/3}$ dependence of the CRSS appearing in both is frequently observed in solid solutions at low temperatures but they leave unsolved the problem of the temperature dependence of the yield stress.

2.4 Thermal effects

Reference to Fig. 3 shows that, excepting the anomalies in face-centred cubic (f.c.c.) metals and alloys usually observed at temperatures below about 70 K (curves b–d), the yield stress of metallic solid solutions is in general found to decrease with increasing temperature up to a certain temperature $T_p \approx \frac{1}{3} T_{melt}$ (curve a), e.g. 400 K in binary copper alloys; at higher temperatures the yield stress is almost temperature independent, and a plateau in the yield stress versus temperature relation is generally observed, indicative of diffusional forms of thermal recovery.

Labusch *et al.* [12] attempted to incorporate thermal effects into the earlier theory [11], mainly to explain the occurrence of the plateau. Thermal activation was assumed to assist dislocation segments to surmount the pinning obstacles. A typical interaction-force profile of the dislocation, taken from their paper, is shown in Fig. 4. With this, a dislocation approaching a repulsive obstacle from the left would lag behind the average position of the dislocation segment at points just in front of the obstacle (Fig. 5), while it would be ahead of the mean position in regions relatively far from the obstacle. Beyond $y_1(l_0')$ (Fig. 4) no stable position exists, and the dislocation moves beyond $y_2(l_0')$. Thermal activation is possible only in the two intervals $y_1(l_0) < y \leqslant y_1(l_0')$ and $y_2(l_0) < y \leqslant y_2(l_0)$. The activation energies of forward and backward jumps between $y_1(l)$ and $y_2(l)$ are E_+ and E_-, respectively, as shown in Fig. 6. Thermal activation of forward jumps results in a decrease of the population at y_1, but an increase arises due to backward jumps from y_2. At temperatures lower than that of the plateau (Fig. 3), mostly forward jumps occur, while at high temperatures, i.e. corresponding to the plateau, the probabilities of forward and backward jumps become nearly equal for most of the effective obstacles; dislocation movement is then of the Brownian type, i.e. they diffuse across the obstacles with an average drift velocity. The CRSS at a given temperature is then

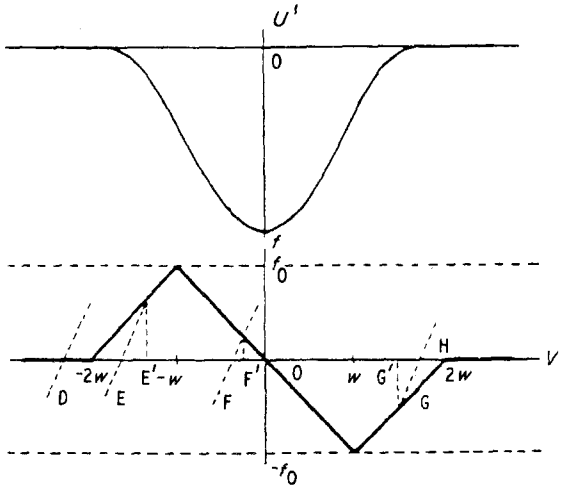

Figure 2 A potential well composed of parabolic arcs, representing the interaction between a dislocation and an obstacle, and the corresponding force–distance curve [18].

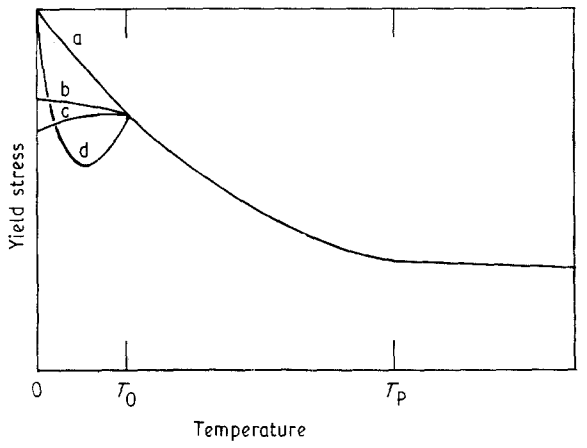

Figure 3 The temperature dependence of the yield stress of solid solutions (schematic) [47].

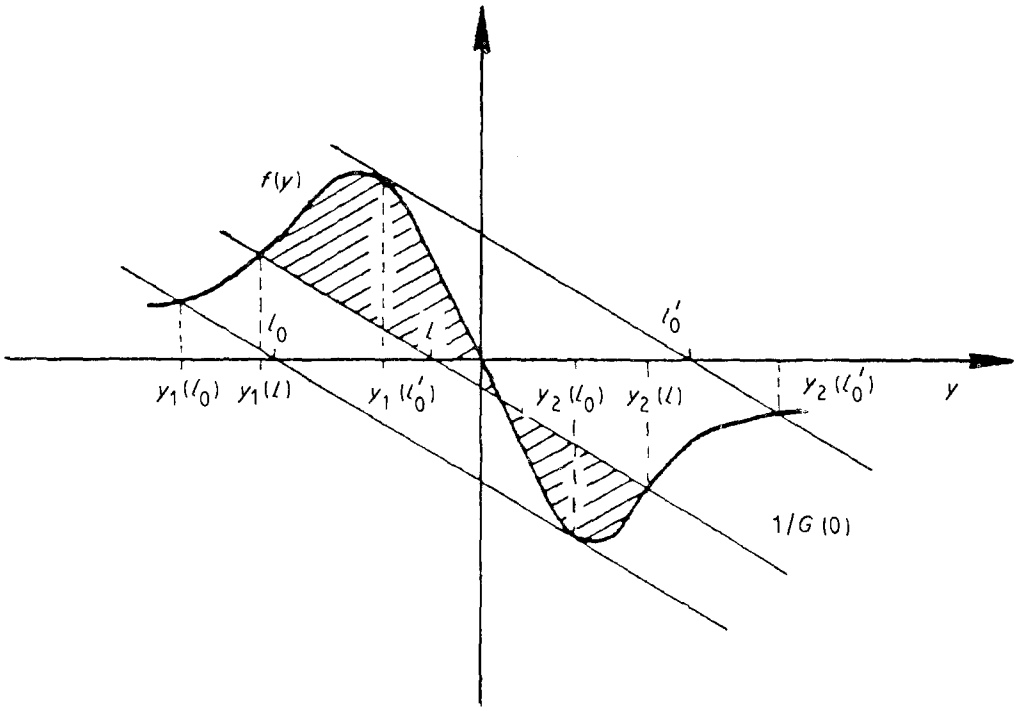

Figure 4 Force–distance relation for an obstacle in the slip plane, and the graphical determination, by the straight line of slope $1/G(0)$, of the equilibrium positions, e.g. $y_1(l_0)$, $y_2(l_0)$, of a dislocation with mean position in the y-direction at l_0 (or at l, l_0'). Shaded areas measure the work done in moving this dislocation between various positions [12].

evaluated as the stress required to "drive" a single dislocation with a prescribed mean velocity $\bar{v}$. This picture is severely simplified compared with that observed by transmission electron microscopy (TEM). For example, the velocity of a single dislocation, observed by TEM during *in situ* creep deformation of specimens of Al-1 at% Mg alloy at a tensile stress of 7.6 MPa at 573 K, can vary over several orders of magnitude, and this is particularly noticeable with dislocations across sub-boundary networks [72]. Also, as Strunin [73] commented, the macroscopic yield strength of an alloy crystal cannot be equated simply to the external stress necessary to lead to a given mean velocity of the dislocations, because as dislocation multiplication proceeds, the mutual interaction of dislocations should be taken into account in deriving values of macroscopic-flow parameters of the solution-hardened materials, i.e. one is dealing with a process involving stochastic interactions. The expression for the yield stress obtained by Labusch *et al.* [12] is

$$\tau = \frac{1}{b}(f_m^4 c^2 w/E)^{1/3}\psi(\theta_0, \omega) \qquad (8)$$

where θ_0 is a dimensionless "reduced" temperature ($\theta_0 =$ constant $\times T$) and ω a "reduced dimensionless velocity" of a dislocation ($\omega =$ constant $\times \bar{v}$). The fraction-term has the same significance as in Equation 5, to which it "reduces" as $T \to 0$ K, when, also, $\psi(\theta_0, \omega) \to A$. The ψ-term decreased with increasing T. According to Equation 8, the τ/T curve levels out to a plateau at temperatures where, for a given rate of deformation, the frequency of back jumps of dislocations become comparable with that of forward ones.

The stress level given by Equation 8, i.e. the height of the plateau, is rather sensitive to the velocity of the dislocations; experiment shows that the plateau level varies but inappreciably with the strain rate to which the crystal is subjected [74, 75]. It is impossible to assume *a priori* a direct relation between dislocation velocity and the strain rate at which the crystal flows; thus, the question of the validity of their theory remains, at best, open. With a stochastic interpretation of the creep processes occurring in the plateau region of temperatures, the assumption that a relation for the strain rate in shear of the type $\dot{\gamma} \propto \exp(-u^*/kT)$ was applicable and that the most probable heights of energy barriers, u^*, determining the rate of plastic flow were given by $u^* \approx mkT$, with m-values in the range 25 ± 2.3 (e.g. [37]) could explain the observed, relatively low dependence of the strain rate on temperature, for $\dot{\gamma}$ would then be nearly independent of T. Also, the level of the plateau stress could be influenced by age hardening of the crystal, an effect not allowed for in the theory. The $c^{2/3}$ dependence of the CRSS, indicated by Equation 8, and already deduced (Equation 5), is often observed at the plateau temperature, e.g. [76, 77]. In fact, as $\psi \neq \psi(c)$ (Equation 8), it should hold for any T; but this is not, in general, found to be the case [9, 62, 74, 75]. The $c^{2/3}$ dependence of the yield stress also appears in Equation 5, which holds only as $T \to 0$ K, and does not, as such, serve as corroboration of the validity of the assumed processes of thermal activation, subsumed within $\psi(\theta_0, \omega)$ in Equation 8.

2.5. Stress equivalence

A rather critical test of the viability of any theory of SSH is the correct description of the CRSS, $\tau(c, T)$, as well as of the activation volume $v(c, T, \tau)$ and, *inter alia* its explanation of the well-established observation

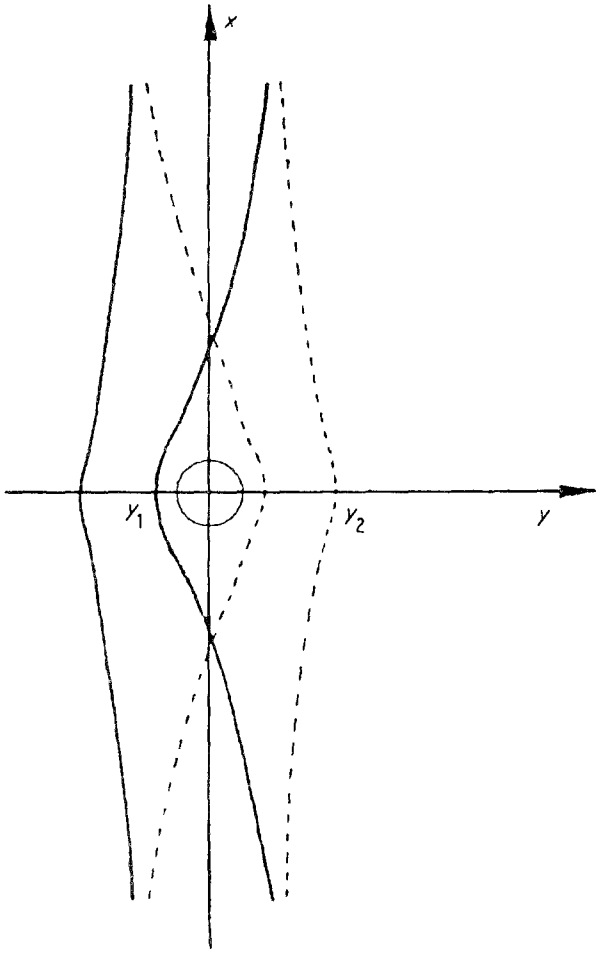

Figure 5 Equilibrium positions of a dislocation moving from $y_1 \rightarrow y_2$ near an obstacle located at the origin [12].

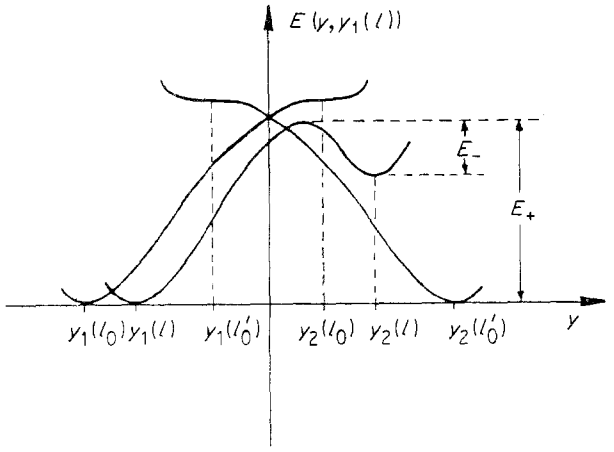

Figure 6 Energy profiles of a dislocation moving along the y-direction between equilibrium positions y_1, y_2, for various mean positions, l, of the dislocation. E_+ and E_- are the activation energies for forward and backward movements, respectively [12].

of stress equivalence (e.g. [27, 30, 33, 40, 78]), i.e. the overlap of the τ/T curves of two solid solutions with the same base but different types and concentrations of solutes. In his papers, Nabarro [21–23] has suggested that stress equivalence of SSH is in part explicable on the basis of the versions of the SSH models of Labusch [11] and Nabarro [18] advanced in the 1970s, although there are clear discrepancies between the observed and the theoretically expected temperature dependences of the flow stress [22]. In the models referred to, the length of the dislocation segment involved in the unit activation process and the CRSS at 0 K, are governed by the parameters cf_m^2 and w (see Equations 5–8), where f_m, as before, is the maximum force of interaction between a solute atom and a dislocation, and w is the range of this force. The parameters cf_m^2 and w appear as a ratio in the expression for the length of dislocation segment, and as a product in that for the CRSS as $T \rightarrow 0$ K [21]. Thus two solid solutions of different solutes in a given solvent metal will have the same values of τ_0(CRSS at 0 K) if $(cf_m^2)_1 = (cf_m^2)_2$ and $w_1 = w_2$. (This is analogous to the stress-equivalence criteria of the nucleation theory of SSH, to be discussed in Section 3). However, if the low-temperature anomaly occurs, then two solid solutions with the same respective values of cf_m^2 and w will not necessarily be stress equivalent in the low-temperature τ/T-anomaly regions unless a further criterion is also met; we shall refer to it in Section 3.6.

Similarly, the stress dependence of the activation volume in copper-and silver-based alloys at $T \rightarrow 0$ K, as derived by Nabarro [21], does not correlate with that observed at 78 and 298 K by Basinski *et al.* [78], Nabarro's theoretical value of the exponent p in the relation $v \propto \tau^{-p}$ is $\frac{1}{2}$ in the "Labusch regime", where $(w/b)(2cE/f_m)^{1/2} > 1$, i.e. one has concentrated solid solutions and weak obstacles. Again, in the "Friedel limit", where $(w/b)(2cE/f_m)^{1/2} < 1$, i.e. dilute solutions and strong barriers, he finds $p = 2$. The corresponding observed values are, however, $\frac{2}{3}$–1 for copper alloys, and $\frac{2}{3}$ for silver alloys in the Labusch regime; the data are equivocal for the Friedel limit. Also, the abrupt vertical step expected by Nabarro [21] in the theoretical v_0/τ_0 curve at rather high stresses, due to a change from a regime in which the two partials of a dissociated dislocation move in a coordinated manner to a regime in which the partials move independently, is not observed experimentally [78, 79].

Nabarro [22] later derived a power law for the stress dependence of the activation volume ($v_0 \propto \tau_0^{-2/3}$), which yielded a better fit in the Labusch regime than the earlier one ($v_0 \propto \tau_0^{-1/2}$). However, the theoretical value of $\Delta v = v(298) - v(78)$ due to the change in temperature (298⇋78 K) at a given stress level, was found to be smaller than the theoretical one by a factor of about three in the case of silver-based alloys, and was even negative for copper-based alloys. As remarked by Nabarro [22], this suggests that the Labusch–Nabarro models referred to did not account adequately for the temperature dependences of the CRSS and of the activation volume.

2.6. Groups of pinners

In an interpretation of the τ/T and related v/T data appertaining to copper single crystals alloyed with either manganese (0.4–7.6 at %) or germanium (0.5–3.3 at %), Wille *et al.* [25] postulated a discrete-barrier model for the onset of yielding, which comprised a field of point-like barriers randomly distributed over the slip planes, with a spectrum of

strengths. They used a Cottrell-Bilby potential of interaction of dislocation with single point-barriers, assuming it to also be applicable to barriers consisting of clusters of solute atoms. Such clusters, e.g. doublets, triplets etc, rather than individual solute atoms, play a central role as effective pinners in the model. Using the Fleischer–Friedel expression [3–5] for the force necessary to move a dislocation across a dilute field of statistically distributed barriers, they deduced that the effective-barrier concentration was less by up to two orders of magnitude than that of the individual manganese or germanium atoms on the dislocations. These low concentrations of the effective barriers were taken by them as justification for the use of concepts embodied in Friedel's treatment of SSH [3] applicable only to relatively dilute solid solutions. However, that model, involving unpinning from single solute atoms in dilute alloys, presupposes weak obstacles; and, hence, it presupposes yielding at low stresses, so that its use with relatively concentrated alloys, where pinners (solute atoms) on dislocations would be but a few interatomic spacings apart, seems hard to accept. In fact, computer simulation of thermally activated dislocation motion (reviewed, for example, by Arsenault and Cadman [71]) showed that with an average dislocation velocity of about $10\,\mu m\,s^{-1}$, and weak obstacles (i.e. the angle between the dislocation arms at the point obstacle being taken as 159°) Friedel's model would be expected to cease to hold at concentrations of single random barriers in excess of about 150 p.p.m., implying a spacing of about 100 lattice spacings between point barriers on dislocations. Also, it is difficult to accept that the pinning of dislocations by isolated solute atoms dispersed between the clusters can be ignored from the point of view of SSH, even though the clusters are assumed to be more strongly bound to the dislocations than the individual point defects [25]. Arsenault and Cadman [71], in a study of the joint effect of randomly distributed barriers of two different strengths on the thermally activated motion of dislocation by computer simulation, found a synergetic effect resulting from coupling between the weak and strong barriers, such that the activation energy necessary to maintain the dislocation velocity in the presence of the weaker pinners in the binary alloy was increased to a value exceeding that for just strong barriers.

2.7. Recent computer simulation

In Labusch's recent treatment by computer simulation [24] of the glide of a "vibrating-string" dislocation in solid solutions allowance is made, in addition to stresses due to dispersed solute atoms, for fluctuating thermal stresses which, for the purpose of computer simulation, are represented by point forces acting on the dislocation on a fine space–time grid. Although the dislocation velocities considered by Labusch were of the order of $100\,m\,s^{-1}$, i.e. unrealistically high compared with the actual velocities which are usually of the order of a few micrometres per second, the model showed some of the features already embodied in the slip-nucleation theory [20] of SSH; in particular, the energy profile along the dislocation path (Fig. 7) indicated that several obstacles were involved in a single event of activation and that with increasing temperature activation areas became progressively larger. However, in its present stage of evolution, Labusch's model [24] does not facilitate the making of detailed comparisons with experiment, although, as with Nabarro's work [22], it points clearly to the need to search for other variants of rate-determining processes; the glide through dispersions of random barriers, although illuminating, did not yield a quantifiable formulation of SSH.

3. Slip-nucleation at barriers of aligned solute atoms

A model of a different type, based on nucleation, rather than on propagation of slip, as the rate-determining process in yielding, was proposed in 1968 by Feltham [8] to account for the temperature and concentration dependences of the CRSS of fairly concentrated solid solutions, i.e. in which the mean spacing of solute atoms on a dislocation was assumed to be only

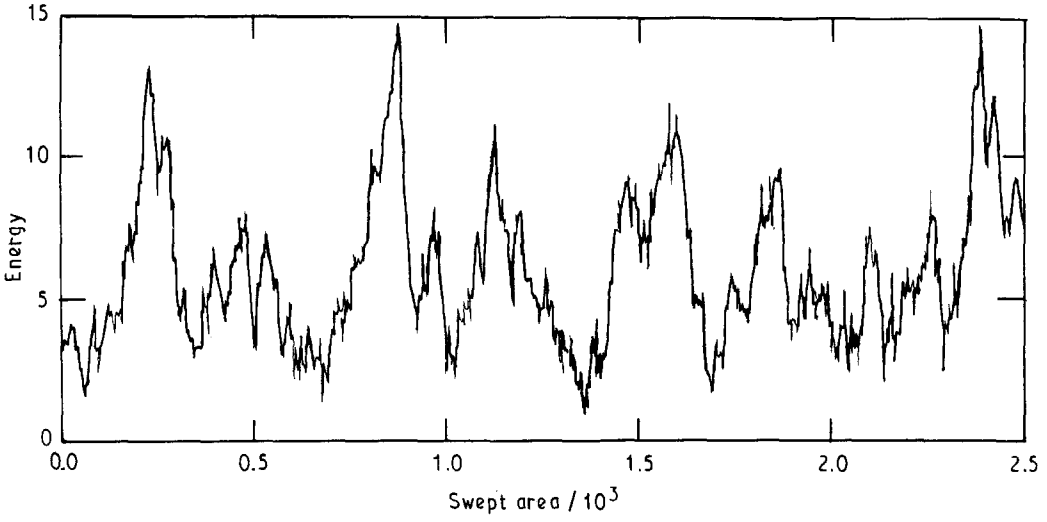

Figure 7 The energy profile along the path of a dislocation in a field of weak obstacles for a sequence of stable positions of minimum energy with saddle-point configurations between them which have to be overcome by thermal activation [24].

a few interatomic spacings. Thus collective breakaway, rather than either an Orowan bypass mechanism, or a Friedel-type unpinning at a single point, was considered. Although initially meant for concentrated solid solutions of metals with low Peierls potentials (i.e. mainly f.c.c.), the functional forms of the nucleation model of SSH [8, 19] was found to have a broader scope, being seemingly applicable to slip nucleation in dilute f.c.c. alloys (with c as low as 0.01 at %) [e.g. 26–28] as well as in hexagonal close packed (h.c.p. e.g. [33, 40, 68]) and body-centred cubic (b.c.c. e.g. [38, 43, 44, 67]) crystals with solute concentration ranging from 0.005 to 45 at %. It leads to dependencies between the variables (CRSS or yield stress, activation volume, solute concentration and temperature) which, being in closed form, are readily verifiable. We shall consider them briefly.

3.1. The basic mechanism

In the paper already referred to above [8], yielding was visualized as occurring as a consequence of the breakaway of edge-dislocation segments from short rows of closely spaced solute-atom pinning points; pinning of screw dislocations was considered too weak by comparison to result in effective barriers to glide. If these barriers are regarded as being "smeared out" over the segment length, rather than localized (Fig. 8), the manner of breakaway can be seen to be somewhat similar to the "kink-pair mode of escape" of dislocations from a Peierls barrier [80]; however, in view of its relatively large length, self-stresses (e.g. kink–kink interactions) are ignored. The mean spacing between neighbouring alloy atoms (denoted by circles in Fig. 8) on a dislocation is taken to be $\lambda \approx b/c^{1/2}$. To facilitate slip under an applied shear stress, the maximum displacement nb of a dislocation segment of length $L(=\mathrm{AB})$, shown in Fig. 8, must suffice to free an arc (ACB) from the short-range stress field of the initial pinning points, to extend the length L to that of the bulge ACB, and to permit its repinning after attainment of the saddle-point configuration in the forward movement.

A simple model of the breakaway of a straight-edge-dislocation segment from a row of mutually non-interacting solute atoms [81] yields approximately $r_0/3^{1/2}$ for the mean displacement $x(=\frac{1}{2}nb)$ into the saddle configuration (Fig. 9), where r_0 is the dislocation core radius. On taking $r_0 = 3b$ as a typical value [82], the relation $\frac{1}{2}nb = r_0/3^{1/2}$ then yields $n \approx 4$. In conformity with this estimate, Feltham [8] estimated that, on average, the critical mean height of the arc ACB (i.e. $\frac{1}{2}nb$) in close-packed metals would be about

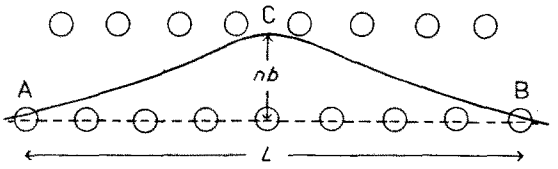

Figure 8 Movement of a dislocation segment to a new pinning site in a stress assisted, thermally activated process (schematic). Circles denote solute atoms [8].

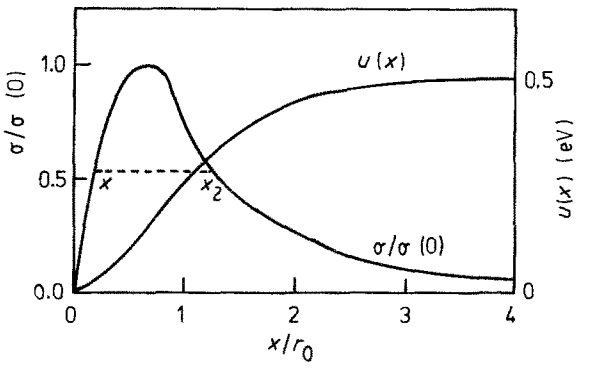

Figure 9 Interaction energy of, and stress on, a dislocation displaced by x in the slip direction from its initial position ($x = 0$) with respect to a line of solute atoms [81]

2–3b, i.e. $n \approx 4$–6; n was not expected to be appreciably dependent on the solute concentration, c. These typical values of n are found in practice, e.g. in the case of f.c.c. (e.g. [26, 30]) and h.c.p. (e.g. [40]) alloys; not unexpectedly, a slight concentration dependence ($n \propto c^{-1/6}$) is observed. However, in the case of b.c.c. metal crystals with high intrinsic lattice friction (high Peierls force) one would expect somewhat smaller n-values. This inference is borne out by observations; values of 1–2 have been found [44], and will be referred to later.

Now, the activation energy W for the passage of the dislocation segment AB between consecutive equilibrium positions, i.e. for the formation of the bulge ACB (Fig. 8), approximated in [8] by a triangle, is given by

$$W = Uc^{1/2}\frac{L}{b} + n^2Gb^3\frac{b}{L} - \tfrac{1}{2}n\tau b^3\frac{L}{b} \qquad (9)$$

where τ is the CRSS at the temperature, T, at which the experiment is carried out, U is the energy expended per solute atom in the process of nucleation of a bulge of critical mean height $\frac{1}{2}nb$ (the saddle configuration), i.e. in the initial breakaway of a dislocation segment from a group of such aligned pinners, and G is the appropriate shear modulus. The saddle point or n-value is difficult to determine with precision, because the interaction of the segment with solute atoms in its passage to the critical configuration has not been adequately solved. However, an estimate based on a well-known model of Cottrell and Bilby [81] suggests that typically $n \approx 4$ [26], as pointed out earlier. The terms on the right-hand side of Equation 9 represent, from left to right, respectively: (i) the energy required for unpinning from the solute atoms close to the dislocation segment AB, (ii) the increase in the total line energy due to formation of the "triangle" ACB from the initial length $L(=\mathrm{AB})$, and (iii) the work done by the applied shear stress in moving the dislocation from AB to ACB.

On denoting the radius of curvature of the arc by R then, as $\tau = Gb/2R$ and $2nbR \simeq L^2/4$, one obtains

$$L/b = (4Gn/\tau)^{1/2} \qquad (10)$$

If the unpinning is to take place at an observable rate ν then, taking ν to be of the order of 0.1–10 s^{-1} to result in plastic deformation at the shear rates ($\dot{\gamma}$) usual in tensile tests, the Boltzmann relation for the

corresponding relaxation times (ν^{-1}), determining the shear rate, $\dot{\gamma}$, is

$$\nu/\nu_0 = \exp(-W/kT) \quad (11)$$

with ν_0 a vibrational frequency of the order of $10^{11}\,s^{-1}$, and $W(\tau)$ the stress-reduced barrier height. On taking logarithms of both sides, one obtains the yield-criterion:

$$W(\tau) = mkT, \quad (m = \ln(\nu_0/\nu) \approx 25 \pm 2.3) \quad (12)$$

where m and its range define the observation window [37], i.e. the range of W values participating in the process.

A feature of the computer simulation of Arsenault and Cadman [71], particularly instructive in relation to the nucleation model, was that, in general, a dislocation pinned along its length moved ahead by the initial nucleation of a small bulge, facilitated by 'unzipping' at a few solute atoms along the dislocation line, normally to its direction of motion. During and after this bulge-out stage of nucleation the side parts of the bulge, while moving more or less parallel to the dislocation line, also advanced normally, taking the dislocation forward a few lattice spacings. The process closely resembles the transition of a dislocation segment from a "necklace" of pinning points to a similar, parallel one through a distance of several Burgers vectors, as was visualised in the nucleation model of SSH in concentrated alloys (Fig. 8) [18, 19]. Yielding is initiated by the thermally activated, stress-assisted breakaway of a straight dislocation segment of length $L(T)$ from an array of pinning points spaced $b/c^{1/2}$ apart; the concomitant increase in the length of the escaping segment facilitates the nucleation of a bulge, somewhat akin to a kink pair, with a mean displacement of about $\frac{1}{2}nb$. At the CRSS, n attains the critical value referred to, i.e. on reaching the saddle configuration. Further unzipping at the corners of the bulge, accompanied by repinning at its leading edge, completes the advance of the dislocation to the new equilibrium position.

It is worthy of note that a characteristic feature of the nucleation model is the inclusion in the energy $W(\tau)$ of a contribution, allowing for the increase in length of the segment in the course of nucleation, in addition to the work expended in the unpinning *per se*. The unzipping at the end points, in the post-nucleation growth stage of the area of slip, would require a low activation energy compared with $W(\tau)$, and would not be rate determining in the glide process. The work done by the dislocation due to encounters with unaligned solute atoms in the transition between two equilibrium positions is not specifically allowed for in the model, but its effect would be expected to appear as contributions to the observed variability of n and U with solute content.

3.2. Temperature dependence of the CRSS

In addition to the specific solute considered, the alloy crystal will usually contain other obstacles to dislocation motion; e.g. Peierls barriers, solid and gaseous impurities, dislocation networks, possibly also point

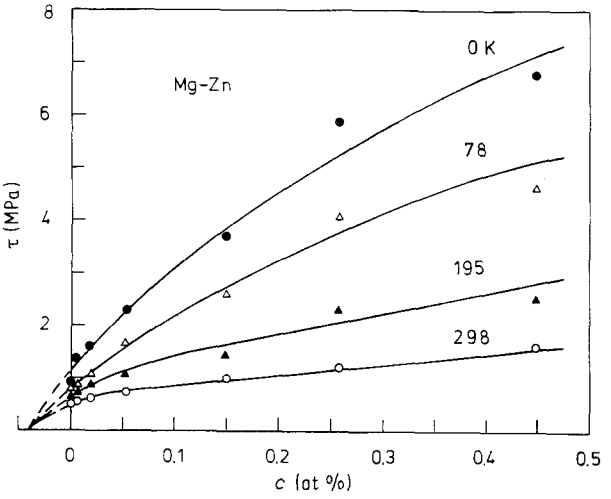

Figure 10 Dependence of the CRSS of Mg–Zn single crystals on alloy content at various temperatures; experimental values, taken from [83], are shown as points. Datra for 0 K were obtained by extrapolation. The equivalent concentration, $c_0 = 0.04$ at % Zn, accounts for the residual stress of the unalloyed Mg crystal [68].

defects in above-equilibrium-concentration and, in particular, conservatively and non-conservatively moving jogs of various lengths and mobilities. The resistance of the alloy crystal to plastic deformation will thereby be enhanced, exceeding the level expected from pinning at the solute atoms only. An effective concentration $c^* = c + c_0$ has then to be used [9, 36] in Equation 9 instead of the nominal solute concentration c; here the "equivalent" concentration, c_0, allows semi-empirically for the presence in the crystal of such drag and pinning barriers. Numerically, c_0 is taken to be equal to the common intercept on the negative c-axis made by the extrapolated τ/c isotherms (Fig. 10). A finite yield stress for $c = 0$, i.e. the resistance of the unalloyed crystal to plastic flow, is thus taken into account. This semi-empirical correction has been found to be of substantial importance in theoretical interpretations of SSH particularly in rather dilute alloys [26, 28, 33, 68], where c_0 is not always negligible compared with c.

The magnitude of c_0 depends on the substructure of the alloy; it is influenced by annealing the crystal and by subjecting the latter to plastic strain. If the crystals were plastically deformed, the τ/c isotherms (Fig. 10) would be displaced upwards along the stress axis, resulting in a larger common intercept on the negative c-axis, as if the solute content had been increased.

Reverting to the nucleation model, the relation for the CRSS, which is now written as $\tau(c^*, T)$, obtained by Feltham from Equations 9–12, then takes the form [8, 9]

$$\tau = \frac{\tau_0 \theta}{[1 + (1 + \theta)^{1/2}]^2} \quad (13)$$

where $\tau_0 (\equiv 4U(c^*)^{1/2}/nb^3)$ is the CRSS as $T \to 0$ K, and $\theta = 4n^2 Gb^3 U(c^*)^{1/2}/(mkT)^2$. We note that the value of U, referring to the displacement of the segment considered only up to the saddle position, should be substantially less than the classical binding energy between a solute atom and an undissociated edge dislocation; for U represents work done as the

segment pulls away from its pinned position to the saddle point ($\approx 14b$), while the binding energy presupposes movement to "infinity". It is regarded as an expectation value; the dispersion originates from short-range modulations of the internal stress field, variations in the edge/screw ratios of the activated dislocation segments, dissociation of the dislocations into partials, as well as from incomplete contacts between pinners and dislocation segments, arising from their limited flexibility.

The energy-of-formation of the bulge (Equation 9, Fig. 8) to which $W(\tau)$ here relates, may also be expressed by the relation [20]:

$$W = W_0(x^{-1/2} - x^{1/2}) \tag{14}$$

where $W_0 = n(U(c^*)^{1/2} Gb^3)^{1/2}$ and $x = \tau/\tau_0$. Then, with the transformation $x = \exp(-2\phi)$, one obtains from Equations 12 and 14: $W = 2W_0 \sinh\phi$, and for sufficiently low temperatures, to which the model applies, (i.e. with $x \to 1$, $\sinh\phi \approx \phi$)

$$W \approx 2W_0\phi = W_0 \ln(\tau_0/\tau) \tag{15}$$

Equation 15, in conjunction with Equation 12, yields $\ln(\tau_0/\tau) = mkT/W_0$ and finally

$$\tau = \tau_0 \exp(-mkT/W_0) \tag{16}$$

a relation generally found applicable in practice [31, 41]. At any given temperature, the CRSS, $\tau(c^*, T)$, thus depends on τ_0 and W_0; U and c^* appear in both parameters only in association, as $U(c^*)^{1/2}$, the effective-binding-energy per unit length of dislocation for transitions from the initial to the saddle-point states.

Equation 16 implies that the slope $\mathrm{d}\ln\tau/\mathrm{d}T$ be constant for a given alloy (Fig. 11), and equal to $-mk/W_0$. The experimental value of $(\mathrm{d}\ln\tau)/\mathrm{d}T$, thus facilitates the determination of W_0, while the point at which the extrapolated $(\ln\tau)/T$ line intersects the stress axis ($T \to 0$ K), denotes the magnitude of τ_0.

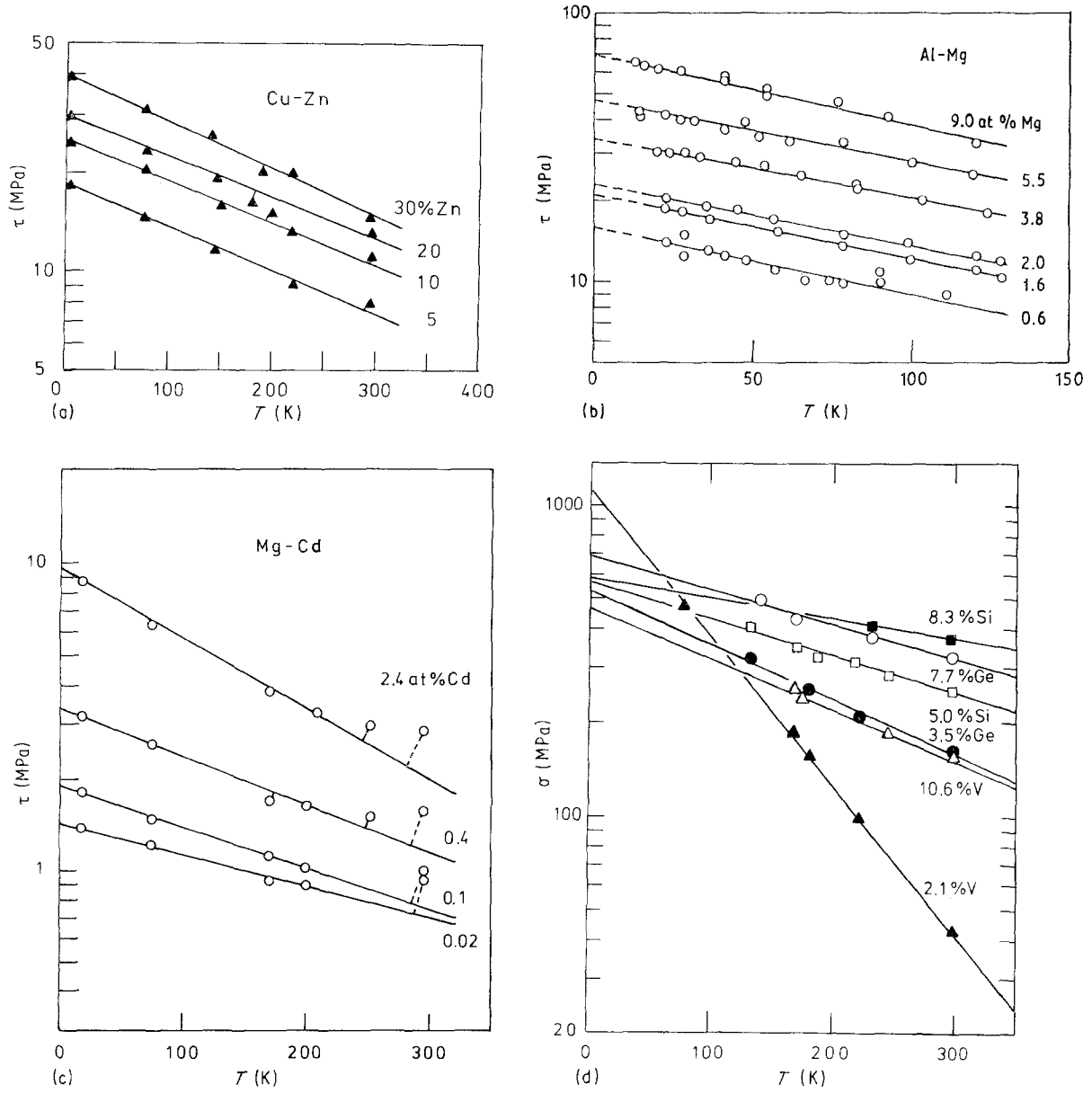

Figure 11 Semi-logarithmic representation of the temperature dependence of the CRSS of (a) Cu–Zn [59], (b) Al–Mg [60] and (c) Mg–Cd [68] single crystals, as well as that of the tensile yield stress of (d) some single crystals of Fe-based alloys [67]. Data points in (a–d) were taken from [84–87], respectively.

Knowing τ_0, W_0 and c^*, n and U can be evaluated by means of the relations [26, 28]

$$n^3 = (W_0^2/\tau_0)[4G/(Gb^3)^2] \quad (17)$$

and

$$U = W_0^2/(Gb^3 n^2 (c^*)^{1/2}) \quad (18)$$

which are readily obtainable from Equations 13 and 14.

3.3. Low-temperature anomalies

Reverting to Equation 16, one finds that the CRSS of a solid solution would be expected to increase monotonically with decreasing temperature. This is observed; however, deviations from this behaviour are frequently found (e.g. [25–27]) below a certain temperature, T_0 (see, e.g., Fig. 12), specific to the alloy. Attempts to account for the anomalies in terms of quantum-mechanical tunnelling and inertial effects, reviewed by Feltham [48], have not lead to convincing interpretations of the observed behaviour. It seems possible that the origin of the anomaly lies in the deformation-induced enhancement of local stresses, to levels above the applied stress, at barriers to the movement of dislocations at temperatures sufficiently low to enable one to neglect structural changes induced by thermal recovery [37, 51]. In close-packed metals the

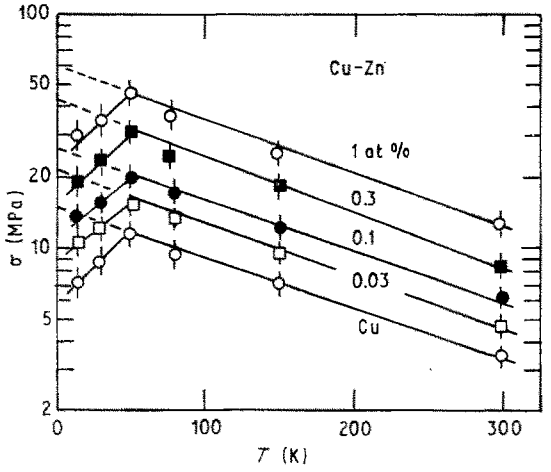

Figure 12 The temperature dependence of the compressive yield stress, $\sigma(=3\tau)$, of polycrystalline copper and brasses of 130 μm grain size, containing up to 1 at % Zn. The results comply with Equations 16 and 19; values of various parameters used are $Gb^3 = 4.6$ eV, $G = 4.5 \times 10^4$ MPa, $n = n_0(c^*/c)^{-0.17}$, $U = U_0\{c^*/c_0\}^{-0.19}$; with $c_0 = 0.04$ at %, $n_0 = 7$, $U_0 = 44$ meV and $T_0 = 50$ K [26].

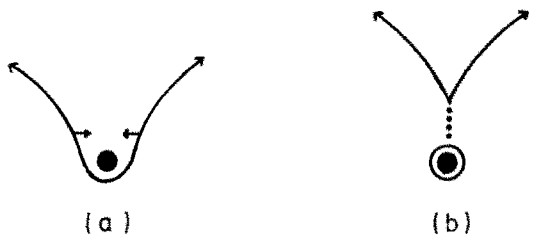

Figure 13 (a) Mutual attraction between two arms of the hairpin in a glide dislocation, leading to (b) an athermal, Orowan, pinch-off; a jogged loop is left around the forest dislocation. Vacancies form at the cusp (jog) of the remaining part of the hairpin.

effect may arise as a consequence of self-stresses of dislocations [37, 88], e.g. due to mutual attraction between two arms of the hairpin in pinch-off configurations at strong obstacles, say forest dislocations (Fig. 13). The applied stress appearing in the kinetic relations of deformation (e.g. τ in Equation 16) has then to be multiplied by a stress-concentration factor $f(T)$ for $T \leqslant T_0$, which for hairpin configurations is estimated to lie between one and four, increasing with decreasing temperature [37]. For $T > T_0$ one sets $f(T) = 1$.

In the case of solid solutions, the arms of the dislocations forming the hairpin, which are of opposite signs, are now impeded in their mutual approach by pinning due to the dispersed solute atoms (Fig. 14); the attractive interaction between the arms is consequently less than that expected with pure metals. This leads to a reduction in the value of $f(T)$ compared with that expected for pure metals. The evidence obtained, e.g. by Feltham and Kauser [26] in the case of dilute brasses ($c = 0.03$–1 at % Zn), lends some support to this proposal; the stress-concentration factor $f(T)$, of the empirical form

$$f(T) = \exp\left(1 - \frac{T}{T_0}\right), \quad (T \leqslant T_0) \quad (19)$$

with $T_0 = 50$ K, accounted for the observations rather well for all solute concentrations (Fig. 12), the lower and upper limits of $f(T)$ were 1 and 2.7, respectively. Evidence of such concentration-dependent reductions in the upper limit of $f(T)$ have also been obtained by Butt and coworkers in the case of Cu–Zn ($c =$ 12–35 at % Zn) [41], Cu–Mn (0.11–7.6 at % Mn) [89], Cu–Al (0.5–14 at % Al) [27, 90], Cu–Ge (0.66–2.95 at % Ge) [70] and Al–Mg (0.6–9 at % Mg) [47, 61].

However, the self-stress of dislocations may not necessarily be the only source of the deformation-induced enhancement of local stresses at temperatures sufficiently low to reduce thermal recovery to comparatively low levels; it could, for example, also be a consequence of structural changes resulting from recovery [51]; thus, below a certain temperature, T_0, thermally activated recovery processes (facilitated, for example, by cross-slip, glide on slip planes parallel or inclined to the most active one, etc) become increasingly inhibited, leading to a concentration of deformation into a few favoured, narrow bands. The internal stresses, for example at unrelaxed pile-ups of dislocations,

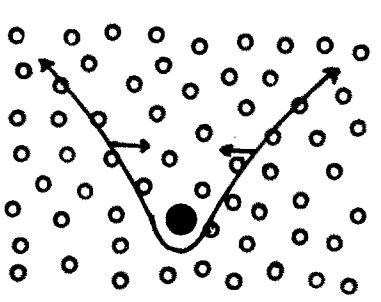

Figure 14 Hairpin configuration of a glide dislocation in the slip plane of a solid solution crystal: (○) solute atoms, (●) forest dislocation. The bulge nucleation occurs at the arms. A loop is left around the forest dislocation, and a jog on the glide dislocation.

would therefore exceed the applied stress in locations where thermally activated processes are most likely to occur. A stress-concentration factor $f(T)$ has then to be used in equations describing the kinetics of the deformation. This view finds some support in observations of mechanical twinning at low temperatures, and in the occurrence of serrated cracks at large strains near grain boundaries, i.e at points of rather high stress [91]. The existence of stress gradients particularly at grain boundaries, and their effect on the slip behaviour of alpha-brass polycrystals, investigated by Hashimoto and Margolin [56], also suggests kindred sources of stress concentrations. Again in a recent paper on computer modelling of the dynamics of spatial dislocation assemblies, Volyntsev [57] shows that where dislocation cell-walls are crossed by slip-bands significant changes take place in the dislocation density, and internal stress concentrations attain a maximum of about four times the level of the applied stress. Dislocation leakage, i.e. local yielding, occurs at such locations.

A different form of the stress-concentration factor $f(T)$ from that given by Equation 19 may sometimes be suitable. Thus the anomaly observed with Cu–Mn single crystals (Fig. 15) has been found to be well encompassed by the stress-concentration factor $f(T)$ of the form [89]

$$f(T) = (T' + T_0)/(T' + T) \qquad (20)$$

where T' = constant, $T \leqslant T_0 \leqslant T'$ and $f(T) = 1$ at $T \geq T_0$ and $f(T) \to 1 + (T_0/T')$ as $T \to 0\,\mathrm{K}$. An interpretation of the dependence of the shapes of the low-T part of the τ/T curves on $f(T)$ in terms of self-stress of dislocations held up at barriers is suggested in [37]. In h.c.p. metals, e.g. α-Ti, Mg, Zn, Co and Be [92–97], the anomaly in the temperature dependence of CRSS for difficult slip systems, i.e. with relatively high Peierls stresses, occurs at rather high temperatures, e.g. 170–450 K for prismatic slip in Be single crystals [97]; as a consequence again, it seems, of the evolution of high local stresses in the course of deformation, but a definitive model is still lacking.

3.4. Temperature dependence of the activation volume

From Equation 14 one has for the activation volume, v, defined by

$$v = (-\partial W/\partial\tau)_T \qquad (21)$$

the relation [19]

$$v = v_0(x^{1/2} + x^{-1/2})/2x \qquad (22)$$

where $v_0 = (1/4)b^3n^2(Gb^3/U(c^*)^{1/2})^{1/2}$ and, as before, $x = \tau/\tau_0$, $\tau_0 = 4U(c^*)^{(1/2)}/nb^3$. With the low-temperature approximation for x given by Equation 16, one obtains from Equations 15 and 21 the simple expression [27]

$$v = v_0 \exp(mkT/W_0) \qquad (23)$$

This, together with Equation 16, and W_0 as given in Equation 14, then yields the hyperbolic relation

$$\tau v = \tau_0 v_0 = W_0 \qquad (24)$$

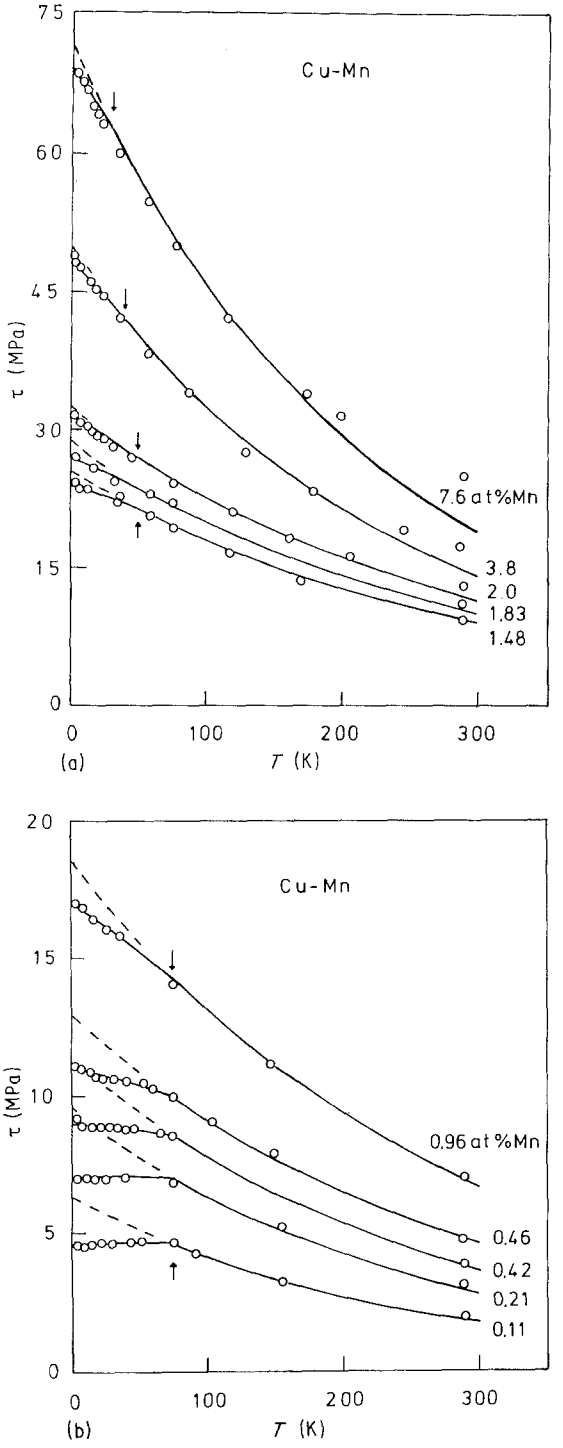

Figure 15 The temperature dependence of the CRSS of Cu–Mn single crystals. The data points are described by Equations 16 and 20; the arrows indicate the critical temperature, T_0, at which the anomaly sets in [89].

Experimentally, the strain-rate sensitivity of the CRSS, defined by $s = T^{-1}(\partial\tau/\partial \ln\dot{\gamma})_T$, rather than v (Equation 21), is determined e.g. by strain-rate cycling experiments [25, 78]; a parameter v_d, with the dimensions of volume, is then evaluated using the relation

$$v_d = kT(\partial \ln\dot{\gamma}/\partial\tau)_T \qquad (25)$$

where $\dot{\gamma}$ is the shear rate of the crystal, expressed by [19]

$$\gamma = \dot{\gamma}_0 \exp(-W/kT) \qquad (26)$$

The pre-exponential factor $\dot{\gamma}_0$ is usually of the order of $10^7\,s^{-1}$ (see e.g. [2, 19]), and taking $\dot{\gamma} = 10^{-4\pm1}\,s^{-1}$ as a typical shear rate, one finds from Equation 26

$$W(\tau) = mkT, \quad (m = \ln(\dot{\gamma}_0/\dot{\gamma}) \approx 25 \pm 2.3) \qquad (27)$$

which is akin to Equation 12. Then, provided the stress dependence of $\dot{\gamma}_0$ is negligible compared with that of $\exp(-W/kT)$, one has from Equation 26

$$kT(\partial \ln \dot{\gamma}/\partial\tau) = (-\partial W/\partial\tau) \equiv v \qquad (28)$$

and, given that proviso, one can write

$$v = v_d \qquad (29)$$

Although this is not invariably correct, we shall assume (with due caution) the validity of Equation 29, to facilitate comparison of experimental data (Equation 25) with the theoretical formalism (Equations 22–24). This assumption seems to be justified by the fact that the agreement between the theoretical curve obtained by means of Equation 22 and the data points referring to v_d for a Cu–30 at % Zn single crystal (Fig. 16) is reasonable.

However, the activation volumes given by Equations 21 and 25 will not be equal if pronounced structural changes occur during strain-rate cycling. Thus Fig. 17 shows that, while the agreement between the experimental τ/T data-points appertaining to some copper-based alloys, obtained by Basinski *et al.* [78], and the theoretical curves (Equations 16 and 20) is rather good over the entire range of temperatures, there are pronounced discrepancies in the case of the temperature dependence of the activation volume at

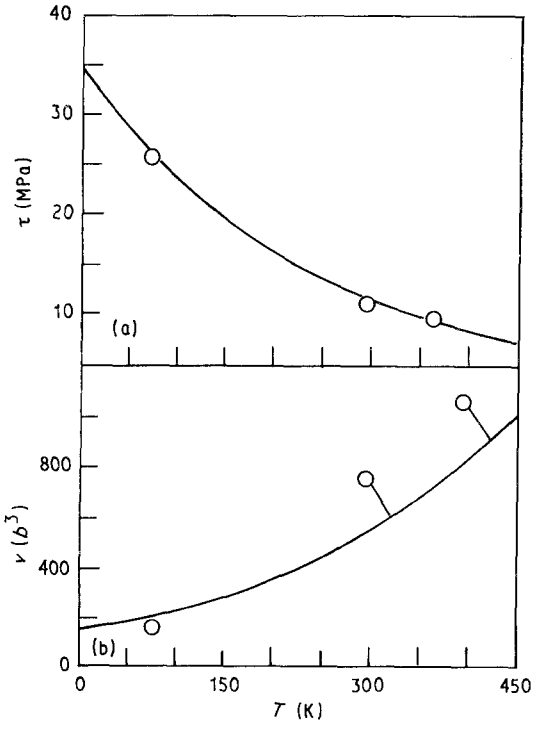

Figure 16 The temperature dependence of the CRSS and of the activation volume for monocrystalline 70/30 brass. Points represent measurements of Traub *et al.* [74]; curves drawn through the data points agree with Equations 13 and 22, in which the values of various parameters used were: $\tau_0 = 35$ MPa, $v_0 = 153b^3$, $c = 30$ at %, $G = 4.5 \times 10^4$ MPa, $Gb^3 = 4.6$ eV, $U = 7$ meV and $n = 4.2$; c_0 was ignored, being negligible compared with c [58].

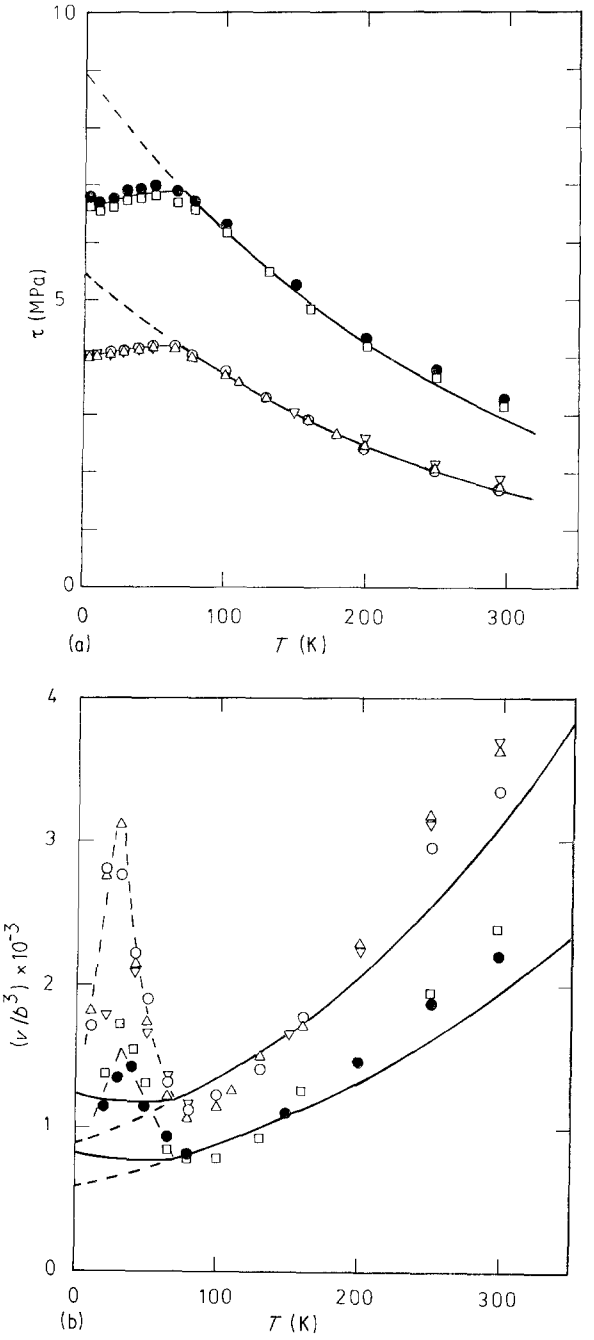

Figure 17 The temperature dependence of (a) the CRSS and (b) the activation volume, for some copper-based alloys. The symbols denote the data obtained by Basinski *et al.* [78]: (●) Cu–0.5 at % Al–0.1 at % Ag, (□) Cu–1.0 at % Al, (△) Cu–0.5 at % Al, (○) Cu–0.1 at % Ag, (▽) Cu–0.5 at % Si. The full curves are theoretical; the points in (b) denote values of v_d (Equation 25) while the curves refer to v (Equation 21). A stress-concentration factor $f(T)$ (Equation 20) was used in Equations 16 and 23 to encompass the anomalous behaviour below 70 K. Discrepancies in (b) seem to arise from differences between v_d (dynamic) and v (static); this is particularly pronounced in the region of the low-temperature anomaly [27].

low temperatures ($T < 70$ K). These occurred, it seems, mainly because the points of Basinski *et al.* [78] were obtained by strain-rate cycling, thus representing v_d (Equation 25), while the theoretical curves, v, were obtained by means of Equation 23.

3.5. Power laws relating stress, activation volume and solute concentration

In the nucleation model of SSH, the concentration dependence of the CRSS depends somewhat on the

temperature [9]. Thus according to Equation 13, as $\tau \to \tau_0$, i.e. $T \to 0$ K, one has $\tau \propto (c^*)^{1/2}$. However, for temperatures high enough to lead to θ-values significantly less than unity, the denominator in Equation 13 is essentially constant and assuming that neither n nor U vary significantly with c^* over a short range of temperatures close to 0 K, one has approximately, $\tau \propto \theta\tau_0$, both τ_0 and θ being proportional to $(c^*)^{1/2}$ (Equation 13) so that the CRSS becomes linearly dependent on the concentration. Thus, if one writes

$$\tau(T) \propto (c^*)^r \tag{30}$$

the r-values would be expected to lie within the limits of 1/2 and 1; the larger values occurring at the higher temperatures (Fig. 18).

Similarly, the concentration dependence of the activation volume is also a function of temperature [38], as is apparent from Equation 22 if written in the form

$$v = \tfrac{1}{2}v_0(\tau/\tau_0)^{-1/2}[1 + (\tau_0/\tau)] \tag{31}$$

As $T \to 0$ K, it yields $v \to v_0 \propto (c^*)^{-1/4}$; while for relatively high temperatures, when $\tau_0/\tau \gg 1$ so that $\theta \to 0$, one has $\tau/\tau_0 \propto \theta \propto (c^*)^{1/2}$ (Equation 13), so that $v \approx \tfrac{1}{2}v_0(\tau_0/\tau)^{1/2}(\tau_0/\tau) = \tfrac{1}{2}v_0(\tau/\tau_0)^{-3/2} \propto (c^*)^{-1/4}(c^*)^{-3/4} \propto (c^*)^{-1}$. These relations may be encompassed by writing [38]

$$v(T) \propto (c^*)^{-q}, \quad (\tfrac{1}{4} \leqslant q \leqslant 1) \tag{32}$$

Experimental results (e.g. Fig. 19) sustain these inferences. We note however that close to their respective upper limits, i.e. at high temperatures, the values of the exponents r and q may not be of relevance here, for then diffusional processes participate in the plastic deformation and, hence, Equations 13 and 31 are no longer applicable.

Assuming the validity of Equation 28, an alternative expression for activation volume (Equation 22), obtainable from Equation 13 in conjunction with Equation 25, in terms of θ is [19]

$$v = v_0[\delta + (1 + \delta^2)^{1/2}]^2(1 + \delta^2)^{1/2}, \quad (\delta = \theta^{-1/2}) \tag{33}$$

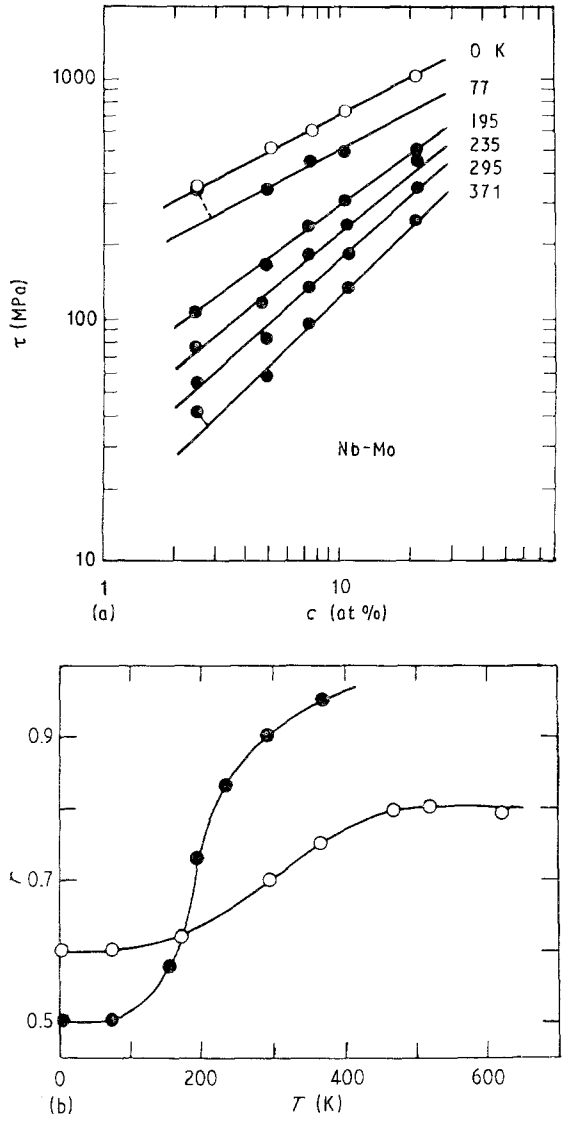

Figure 18 (a) The concentration dependence of the CRSS, τ, of Nb–Mo alloy single crystals as function of temperature. The data points were taken from [99]; those for 0 K represent extrapolated values [44]. (b) The temperature dependence of the exponent r in Equation 30 for (●) Nb–Mo and (○) Ta–Re alloys [44].

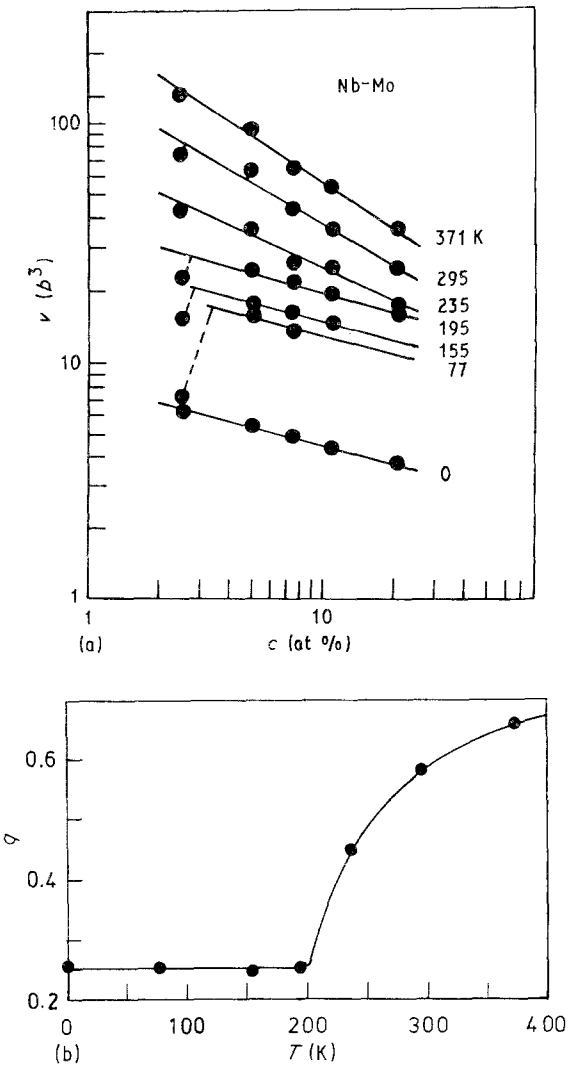

Figure 19 (a) The concentration dependence of the activation volume, v_d (Equation 25), of Nb–Mo crystals. Data points from [99]; values for 0 K were obtained by extrapolation [38]. (b) Values of the exponent q (Equation 32) derived from the slopes of the curves drawn through the data points in (a) as function of temperature [38].

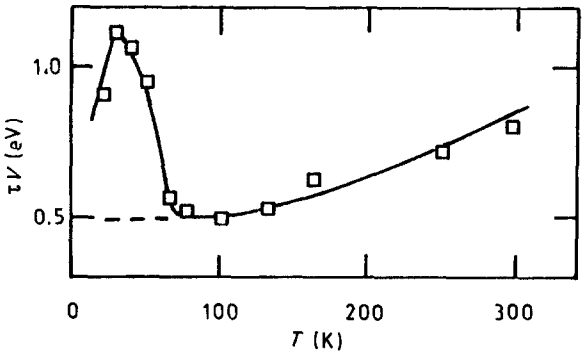

Figure 20 The product τv as function of temperature for a Cu–1 at % Al alloy single crystal, referred to in Fig. 17 [98].

For an alloy at a given temperature Equations 13 and 33 yield

$$\tau v = \tau_0 v_0 (1 + \delta^2)^{1/2} \quad (34)$$

As $\delta = \theta^{-1/2} \propto T$, the product τv for a given alloy therefore increases somewhat with rising temperature. Excepting the anomalous hump below about 70 K (Fig. 20) due to the occurrence of pronounced structural changes during strain-rate cycling, the variation of (τv)-values with temperature in the case of Cu–1 at % Al alloy single crystal is in accord with this expectation. However, at rather low temperatures, i.e. when $\delta^2 \ll 1$, the expression simplifies, as the bracketed term may then be omitted. An alternative form for the product of τ and v, obtainable from Equation 22, in terms of $x(= \tau/\tau_0)$ is [39]

$$\tau v = \tfrac{1}{2}\tau_0 v_0 [x^{1/2} + x^{-1/2}] \quad (35)$$

Hence, as $T \to 0$ K, i.e. $x \to 1$, the hyperbolic relation $\tau v = \tau_0 v_0$, is again obtained (Equation 24), and substantiated by experiment in Fig. 21.

3.6. Stress equivalence

The term stress equivalence refers to a phenomenon first observed by Basinski *et al.* [78]. They found that if two solid solution crystals with differing solute contents but in the same solvent, in this case copper or silver, had the same CRSS at any temperature, here in the range 4–380 K, then their CRSS/T curves were coincident, (see e.g. Fig. 17a). Similarly v_d (Equation 25), obtained by strain-rate cycling, was found to be uniquely related to the CRSS, irrespective of the type of alloying element and its concentration (Fig. 22). Also, for the solid solutions based either on copper or silver, the difference between the CRSS at 78 K and that at 298 K, expressed as a function of the CRSS at 78 K, was independent of alloy type and concentration c, i.e. a single common curve was obtained for all alloy concentrations, and solute types in a correlation of $\tau(78)$–$\tau(298)$ with $\tau(78)$. A corresponding result was also found by Butt *et al.* [40] to apply to other f.c.c., h.c.p. and b.c.c. alloys [19, 69, 76, 78, 84, 100–112] with solute concentrations ranging from 5×10^{-3} to 30 at % (Fig. 23).

Concerning the superimposition of the τ/T curves of solid solutions with the same base but different

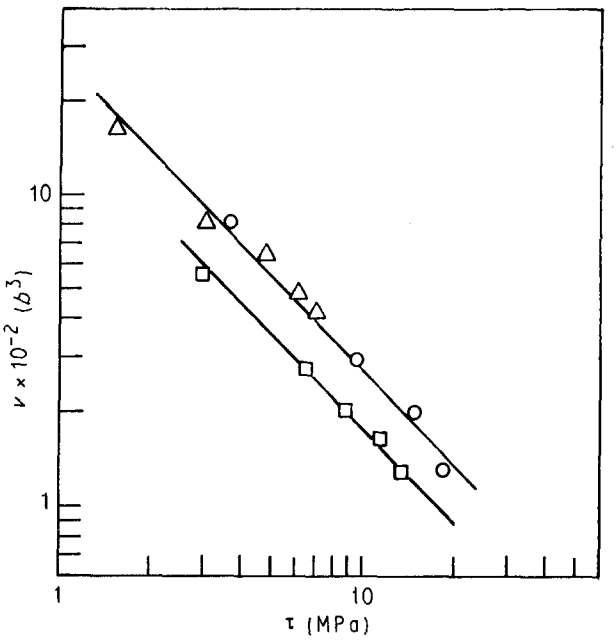

Figure 21 The dependence of activation volume v_d (Equation 25) on CRSS of Mg–Li alloy single crystals. The gradient $(d \ln v_d)/(d \ln \tau)$, of the line drawn through the data points, taken from [107], at a given temperature is -1, as required by Equation 24 [68]: (○) 4 k, (□) 78 K, (△) 198 K.

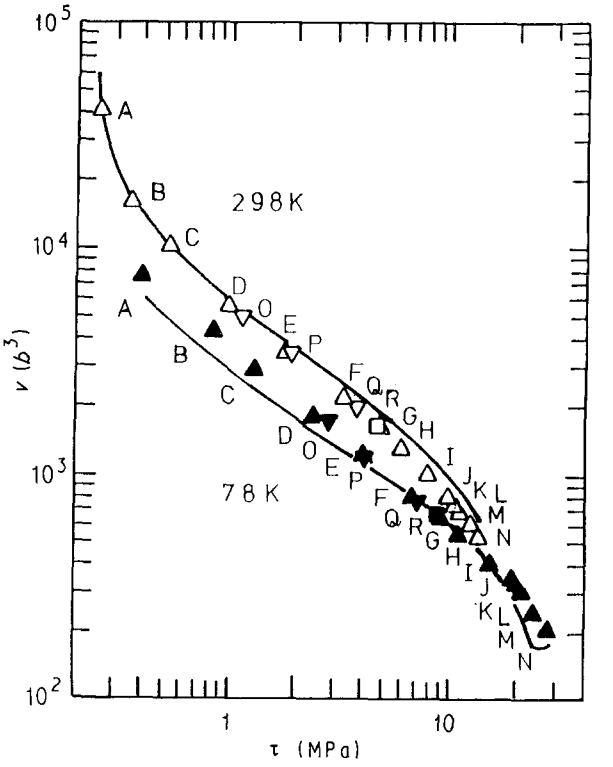

Figure 22 The dependence of the activation volume, v_d on the (concentration dependent) CRSS and on the temperature for (△) Cu–Al, (▽) Cu–Ag and (□) Cu–Ni alloys. The curves represent the experimental data of Basinski *et al.* [78]; the symbols denote theoretical values. The latter were derived by means of Equation 23, using values of τ_0 and W_0, determined from the experimental τ/T data by means of Equation 16. Points A–N refer to copper single crystals, containing 0.01–11 at % Al, points O–Q refer to 0.05–0.19 at % Ag and point R to 5 at % Ni [27].

solutes, i.e. stress equivalence, Equation 16 shows that for stress-equivalence of alloys 1, 2, 3 . . . , one must have

$$(\tau_0)_1 = (\tau_0)_2 = (\tau_0)_3 = \cdots \quad (36)$$

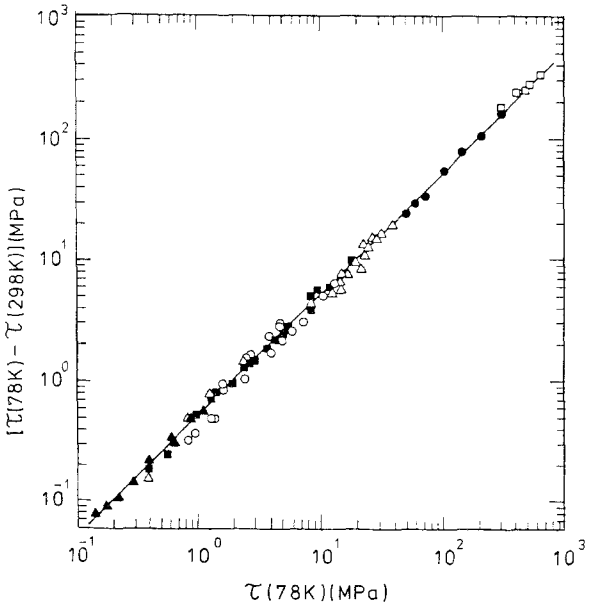

Figure 23 Experimentally established stress equivalence, $\tau(78)-\tau(298)$ versus $\tau(78)$, for several sets of binary alloys. The points lie close to a common single line of unit gradient, as required by Equation 43 [40]. Data for: (□) Nb-based single crystals [100], (●) Ti-based polycrystals [101], (▲) Cd-based single crystals [69, 102, 103], (○) Mg-based single crystals [104–108], (△) Cu-based single- and polycrystals [19, 76, 78, 84, 109] and (■) Ag-based single crystals [110–112].

and

$$(W_0)_1 = (W_0)_2 = (W_0)_3 = \cdots \quad (37)$$

or, in terms of n and U [26]

$$n_1 = n_2 = n_3 = \cdots \quad (38)$$

$$(U(c^*)^{1/2})_1 = (U(c^*)^{1/2})_2 = (U(c^*)^{1/2})_3 = \cdots \quad (39)$$

The values of n and $U(c^*)^{1/2}$ for several copper- and silver-based alloy single crystals given in [27], confirm these criteria. Also, Equations 36 and 37, in conjunction with the relation $\tau_0 v_0 = W_0$ (Equation 24), suggest that solid solutions of different solutes in a given solvent metal, which exhibit the same τ/T behaviour, will also satisfy the condition

$$(v_0)_1 = (v_0)_2 = (v_0)_3 = \cdots \quad (40)$$

and hence such solid solutions would be expected to have a common v/T curve (Equation 23) as well. This inference is borne out by the v_d/T data (Fig. 17), obtained by Basinski *et al.* [78] with copper-based alloys. Note that deviations from the theoretical curves in Fig. 17b appear to be due to differences between v_d (Equation 25), as determined by strain-rate cycling experiments [78], and v (Equation 21). Also, it should be remembered that in the case of stress-equivalent solid solutions in which the CRSS/T anomaly occurs, the condition [26]

$$f_1(T) = f_2(T) = f_3(T) = \cdots \quad (41)$$

has to be added to Equation 36 and 37. Deviations from stress equivalence at low temperatures, suggesting failure of this criterion, have been observed with copper single crystals containing either manganese or germanium in solid solution [25].

Similarly, a relation for the stress equivalence of the difference in CRSS between two temperatures T_1 and T_2 ($T_2 > T_1$), derived from Equation 13, obtained on writing $\theta = (A/T)^2$ for a specific alloy, and readily amenable to experimental study, is [19]

$$\frac{\tau(T_1) - \tau(T_2)}{\tau(T_1)} = 1 - \left[\frac{T_1 + (T_1^2 + A^2)^{1/2}}{T_2 + (T_2^2 + A^2)^{1/2}}\right]^2, \quad T_1 < T_2 \quad (42)$$

For values of T, either rather smaller or larger than A ($=2W_0/mk$), the ratio $[\tau(T_1) - \tau(T_2)]/\tau(T_1)$ may readily be seen to be but little dependent on the alloy concentration. An alternative, simpler, expression for Equation 42 can be obtained on using the low-temperature approximation given by Equation 16, a procedure generally justified within the domain of validity of the nucleation model. One then has [41]:

$$\frac{\tau(T_1) - \tau(T_2)}{\tau(T_1)} = 1 - \exp\left[-\frac{mk}{W_0}(T_2 - T_1)\right] \quad (43)$$

and as, for a given set of binary solid solutions W_0 is not significantly dependent on c, the right-hand side of Equation 43 is constant for a given set of limit temperatures (T_1, T_2), so that one would expect

$$\frac{\delta \ln[\tau(T_1) - \tau(T_2)]}{\partial \ln \tau(T_1)} \approx 1$$

for all solid solutions, as seems to be the case (Fig. 23). Variations of W_0 from one alloy system to another seem to be sufficiently small to result in the confinement of the experimentally determined points into a relatively narrow band around the line of unit slope in the double-logarithmic presentation shown in Fig. 23. A similar correlation can also be shown to hold for $v(T_2) - v(T_1)$ and $v(T_1)$ in accordance with the expression [27]

$$\frac{v(T_2) - v(T_1)}{v(T_1)} = \exp\left[\frac{mk}{W_0}(T_2 - T_1)\right] - 1 \quad (44)$$

Further, for a given change in the test temperature $\Delta T = T_2 - T_1$ one can, by means of Equations 43 and 44, readily find the expression for the product of the accompanying changes in the CRSS, $\Delta\tau = \tau(T_1) - \tau(T_2)$ and the associated activation volume, $\Delta v = v(T_2) - v(T_1)$ [27]:

$$(\Delta\tau)(\Delta v) = 2W_0[\cosh(mk\Delta T/W_0) - 1] \quad (45)$$

Neglecting the weak c-dependence of W_0, the right-hand side of Equation 45 is a constant for a given ΔT. One then obtains for a given set of binary solid solutions:

$$\left.\frac{\partial \ln \Delta\tau}{\partial c}\right|_{\Delta T} = -\left.\frac{\partial \ln \Delta v}{\partial c}\right|_{\Delta T}$$

and hence $\partial \ln \Delta\tau / \partial \ln \Delta v = -1$. Fig. 24 refers to the dependence of $\Delta v_d = v_d(T_2) - v_d(T_1)$ on $\Delta\tau = \tau(T_1) - \tau(T_2)$, for copper- and silver-based solid solutions ((a) and (b), respectively) with $T_2 = 298$ K and $T_1 = 78$ K. The experimental values (strictly v_d not v) of Basinski *et al.* [78] for copper-based alloys have

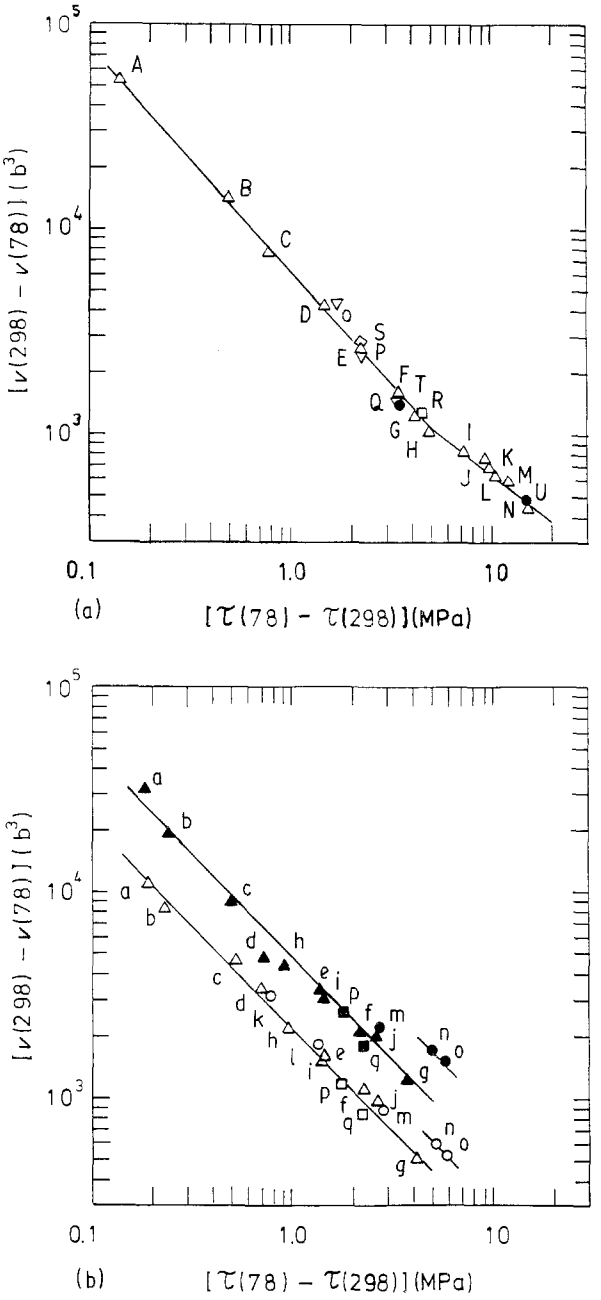

Figure 24 The relation between $v(298)$–$v(78)$ and $\tau(78)$–$\tau(298)$ for (a) copper-based alloys ((△) Cu–Al; (□) Cu–Ni; (▽) Cu–Ag; (◇) Cu–Si; (●) Cu–Al–Ag) and (b) silver-based alloys ((△) Ag–In; (○), Ag–Sn; and (□) Ag–Au). The solute contents, c, ranged from 0.01 to 11 at % in the case of the former, and from 0.01 to 20 at % for the latter series. In (a) the symbols denote the experimental values (v_d) of Basinski *et al.* [78]; as the theoretical values obtained by the use of Equations 43 and 45 are close to the experimental values, they have been omitted. In (b) the filled symbols (▲, ●, ■) represent experimental data (v_d) taken from [78]; the open symbols (△, ○, □) are theoretical, i.e. evaluated by means of Equation 43 and 45 [27].

been denoted by symbols in Fig. 24a. Those derived by means of Equations 43 and 45, being close to the experimental values, were omitted for clarity. Similarly, the full symbols in Fig. 24b denote the data (strictly v_d not v) of Basinski *et al.* [78] for silver-based alloys; the open symbols were determined by means of Equations 43 and 44. Although the points denoting theoretical values of Δv in Fig. 24b are somewhat lower than the experimental ones, most probably due to the differences in v_d (Equation 25) and v (Equation 21) arising from the occurrence of pronounced structural changes during strain-rate cycling, and due to possible diffusional effects operative at room temperature, the slope of the line drawn through the points in each case is equal to -1, as required by Equation 45. Similarly the slope of the curve drawn through the data points appertaining to copper-based alloys in Fig. 24a is also close to the theoretical value of -1.

4. Metals with a high Peierls potential

A close analogy exists between the modes of the escape of a dislocation segment from a Peierls barrier, i.e. by kink-pair nucleation [80], and the breakaway from a row of closely spaced solute atoms [8]. The temperature dependence of the CRSS of b.c.c. metals, which have a high Peierls potential for screw dislocations compared with f.c.c. metals, is more pronounced as a consequence than that of f.c.c. metals, but it is akin to that of relatively concentrated f.c.c. solid solutions. As kink-pair formation similar to the nucleation of a bulge in solid solutions is also considered to facilitate the passage of dislocations over a Peierls barrier, i.e. yielding in b.c.c. metals, a relation of the same form as Equation 13 or 16 could also be expected to account for the temperature dependence of the CRSS of pure b.c.c. metals. In this case U would be interpreted as the Peierls energy per interatomic spacing along the screw dislocation, c^* would be equated to unity [80], and n would be anticipated to lie in the range 1–2 [43, 44]. This hypothesis has in fact been found to account quite well for observations [43–45, 67], as is exemplified by the temperature dependence of the CRSS and of the activation volume v_d (Equation 25) in the case of several b.c.c. metals [46, 87, 113–115], shown in Figs 25 and 26. These results provide further, indirect, support for the nucleation model.

A feature of particular interest arises from the near equality of the lattice spacings and of the valencies respectively of Ta and Nb, as a result of which one may expect solid solution hardening in a Nb–Ta alloy system to be negligible. The coincident values (denoted by points) for all solute concentrations and pure metals in Figs 25 and 26 show that these alloys behave as the pure solvent crystal ($c^* = 1$) with respect to the temperature and concentration dependences of both the CRSS and the activation volume, v_d (Equation 25).

5. Superposition of solid-solution hardening and work hardening

The effect of work hardening on the solution-strengthening mechanism has not yet been extensively explored [39, 116–119]. In 1970 Suzuki [116] studied the problem; he introduced dislocations into copper-alloy single crystals, which had rather low grown-in dislocation densities, by twisting them. Tensile specimens of a certain orientation were cut from the twisted crystals so that the screws introduced into them acted as forest dislocations. He found that below a certain

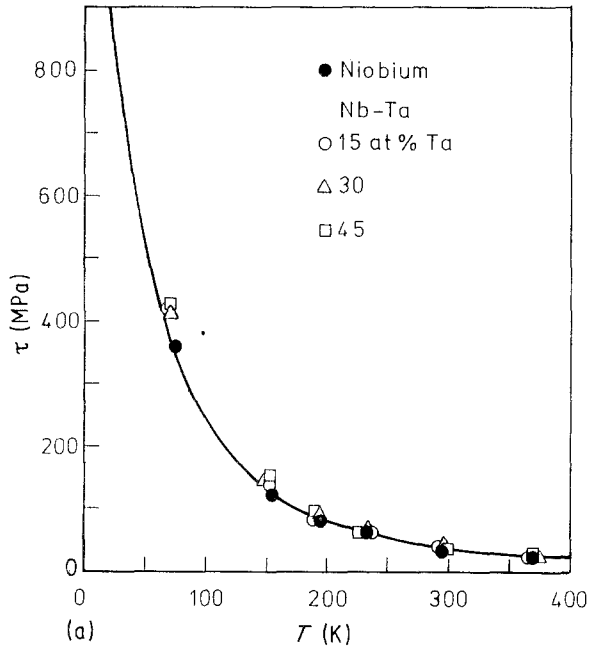

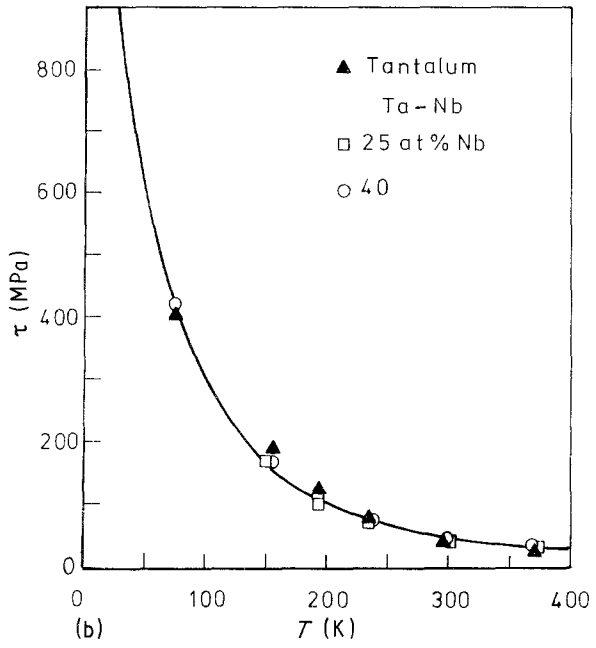

Figure 25 The temperature dependence of the CRSS of atypical (a) Nb and Nb–Ta [114], and (b) Ta and Ta–Nb [113] single crystals. The theoretical curves drawn through the data points comply with Equation 13 with $c^* = 1$ [44].

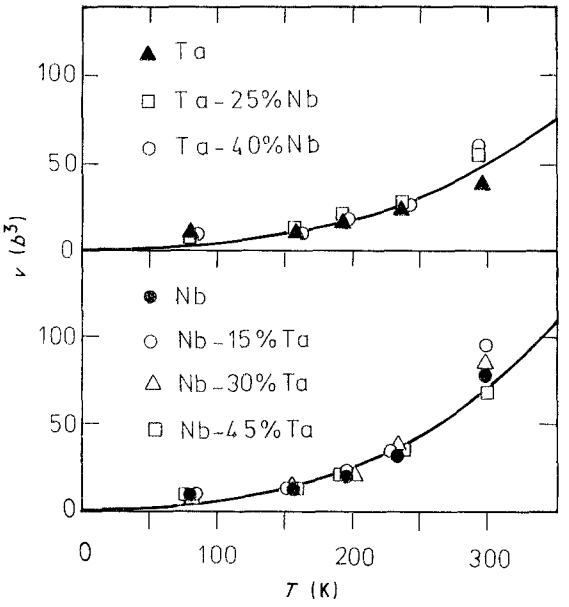

Figure 26 The temperature dependence of the activation volume, v_d, for the metals and alloys referred to in Fig. 25. The theoretical curves encompassing the data points comply with Equation 22, with $c^* = 1$ [44].

critical density of forest dislocations the yield stresses of single crystals of Cu–0.25 at % Ni and Cu–0.17 at % Al at 77 and 300 K were determined primarily by the solute atoms, while, above that critical density, it was determined by the forest, i.e. it was proportional to the square root of the forest density.

Basinski [117] later carried out strain-rate cycling experiments, at room temperature, with single crystals of copper and of a copper alloy containing 0.05 at % Al. The change in the flow stress in shear, $\Delta\tau$, accompanying a given strain-rate change was determined in each case at several stress levels, i.e. going along the stress–strain curve. He observed that $\Delta\tau$ was dependent on solute content at low stresses, i.e. in the early stage of plastic deformation, while at high stresses (shear strain > 45%), the $\Delta\tau/\tau$ curve for Cu–0.05 at % Al coincided with that for copper. Measurements made by Wielke *et al.* [118], between 4 and 50 K, on cadmium single crystals alloyed with 0.01, 0.03, 0.08, 0.28 and 0.7 at % Zn, corroborated Basinski's observations. They found that the activation volume $v_d \equiv kT[\partial \ln \dot{\gamma}/\partial\tau]_T$ decreased with increasing flow stress, and that the initial dependence of v_d on the alloy concentration c disappeared at shear strains greater than about 40%.

We note that the v_d/τ relations obtained by Krasova *et al.* [119] at room temperature with single crystals of Cu–Si solid solutions containing 0.07, 0.23 and 3.26 at % Si coincided, falling on a single smooth curve over the entire flow stress range studied (4–24 MPa). Here too, the independence of v_d on solute concentration seems to be a consequence of the rather large strains at which the activation volumes were determined; work-hardening (WH) rather than SSH then determined the flow stress.

Recently, Butt and Feltham [39] obtained correlations, akin to those of Basinski [117] and of Wielke *et al.* [118] for single crystals, but using polycrystalline copper and brasses (10–30 at % Zn) at 77, 200 and 290 K at compressive stresses, σ, ranging from 30 to 300 MPa, with a maximum compressive strain, ε, of 14%. They found the magnitude of the activation volume

$$v_\sigma = kT(\partial \ln \dot{\varepsilon}/\partial\sigma)_T$$

appertaining to a given stress level and temperature ($\dot{\varepsilon} = 4 \times 10^{-5}\,s^{-1} \leftrightharpoons 4 \times 10^{-4}\,s^{-1}$) to depend on the zinc concentration in the stress range corresponding to compressive strains of less than about 4%; at higher strains it was found to be independent of the solute content.

Also, in a representation of $v_\sigma\sigma$ versus σ, Butt and Feltham [39] observed that for brasses and for copper, the values of $v_\sigma\sigma$ coincided at high stresses, corresponding to compressive strains of more than 4%,

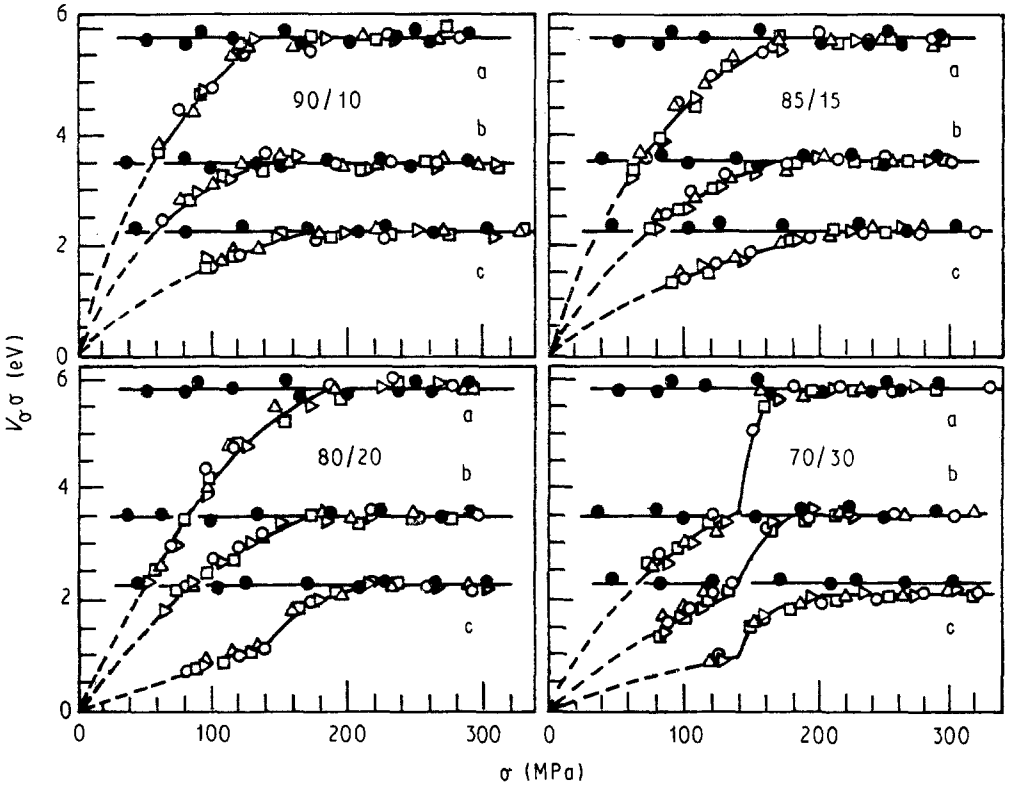

Figure 27 Stress dependence of the product of activation volume $v\sigma = kT(\partial \ln \dot{\varepsilon}/\partial\sigma)_T$ and the corresponding compressive flow stress σ, for brasses of various grain sizes at (a) 290 K (b) 200 K and (c) 77 K. The full circles refer to polycrystalline copper of 99.999% purity [39].

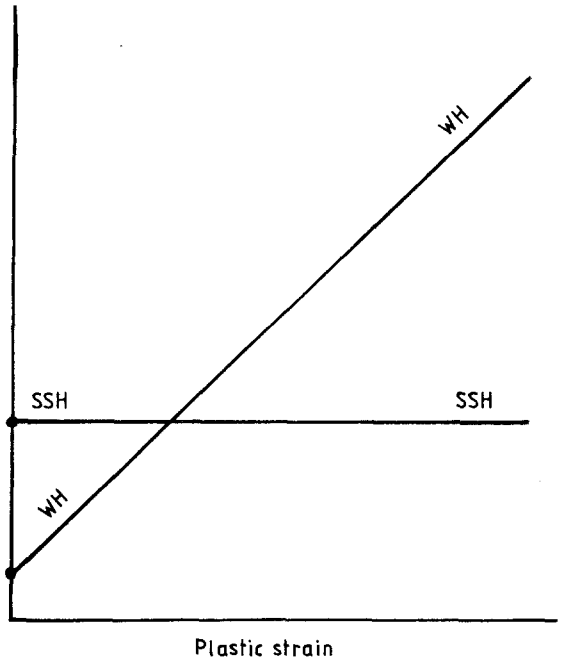

Figure 28 Superposition of solid-solution hardening (SSH) and work hardening (WH) in a solid solution for a given temperature, strain rate and solute concentration (schematic). The effective hardness for any strain is that represented by the higher-lying of intersecting curves for that value of strain; SSH and WH regions are to the left and to the right of the crossover point, respectively.

while at low stresses they did not (Fig. 27). They concluded that alloy atoms are effective obstacles to dislocation motion in the initial stage of plastic deformation, but that beyond certain values of the tensile strain, work hardening became rate determining; resistance of the crystals to plastic deformation then derived mainly from the forest rather than from the alloy atoms, i.e. as indicated schematically in Fig. 28.

6. Conclusions

1. The nucleation model of SSH [8, 19, 31] explains adequately the principal features of the dislocation kinetics involved in solid solution hardening of f.c.c., h.c.p. and b.c.c. alloy crystals, with solute contents down to about 100 p.p.m.

2. It accounts satisfactorily for the principal observed features of SSH. These appertain to the temperature and concentration dependencies of the CRSS (Equations 16 and 30) the activation volume (Equations 23 and 32) the product of activation volume and CRSS (Equations 24 and 34), the stress equivalence (Equations 43 and 45), and the role of hardness of the unalloyed (base) metal (equivalent concentration c_0) on SSH.

3. The anomalies in the mechanical response of solid solution crystals observed below about 70 K are also consistently accomodated by the model (Equations 19 and 20) at temperatures at which thermal recovery is low.

Note added in proof: In a recent paper [120] Feltham and Kauser derived Equation 20, showing that due to the catastrophic breakaway of slip dislocations, initiated as described in Reference 26, there attained "dynamic" velocities, and were consequently subjected to appreciable phonon friction. As the latter decreases with decreasing temperature, the slip-distance lengthens; its magnitude is proportional to "f" as given by Equation 20, which they derive.

Acknowledgement

One of us (MZB) is grateful to the Nobel Laureate Professor Muhammad Abdus Salam and the Swedish Agency for Research Cooperation with Developing Countries for hospitality at the International Centre for Theoretical Physics, Triests, Italy, where most of this work was done during a visit in the capacity of Associate Member. Their financial assistance for a study visit to London to finalize the manuscript is also gratefully acknowledged.

References

1. N. F. MOTT and F. R. N. NABARRO, in "Report of a conference on the strength of solids" (The Physical Society, London, 1948) p.1.
2. H. SUZUKI, in "Strength of metals and alloys", edited by H. J. McQueen (Pergamon, Toronto, 1986) p. 1727.
3. J. FRIEDEL, "Dislocations" (Pergamon, Oxford, 1964) p. 379.
4. R. L. FLEISCHER, Acta Metall. **11** (1963) 203.
5. R. L. FLEISCHER and W. R. HIBBARD, in "Conference on relation of structure to mechanical properties of metals" (National Physical Laboratories, Teddington, 1964) p. 262.
6. B. R. RIDDHAGNI and R. M. ASIMOW, *J. Appl. Phys.* **39** (1968) 4144.
7. *Idem, ibid.*, **39** (1968) 5169.
8. P. FELTHAM, *J. Phys. D: Appl. Phys.* **1** (1968) 303.
9. *Idem., Mater. Sci. Engng.* **11** (1973) 118.
10. R. LABUSCH, *Phys. Status Solidi* **41** (1970) 659.
11. *Idem., Acta Metall.* **20** (1972) 917.
12. R. LABUSCH, G. GRANGE, J. AHEARN and P. HAASEN, in "Rate processes in plastic deformation of materials", (American Society for Metals, Cleveland, 1975) p. 26.
13. O. BOSER, *J. Appl. Phys.* **44** (1973) 1033.
14. *Idem., ibid.* **44** (1973) 1038.
15. *Idem., Acta Metall.* **24** (1976) 439.
16. P. KRATOCHVÍL, P. LUKÁČ and B. SPRUŠIL, *Czech. J. Phys.* B **23** (1973) 621.
17. U. F. KOCKS, R. LABUSCH and R. B. SCHWARZ, in "Fourth international conference on the strength of metals and alloys", Vol. 1, (American Society for Metals, Nancy, France, 1976) p. 275.
18. F. R. N. NABARRO, *Phil. Mag.* **35** (1977) 613.
19. M. Z. BUTT and P. FELTHAM, *Acta Metall.* **26** (1978) 167.
20. *Idem., Rev. Deform. Behav. Mater.* **3** (1978) 99.
21. F. R. N. NABARRO, Proc. Roy. Soc. Lond. **381** (A) (1982) 285.
22. *Idem., Phil. Mag.* **B52** (1985) 785.
23. F. R. N. NABARRO, in "Dislocations and properties of real materials" (The Institute of Metals, London, 1985) p. 152.
24. R. LABUSCH, *Czech. J. Phys.* B **38** (1988) 474.
25. T. WILLE, W. GIESEKE and C. SCHWINK, *Acta Metall.* **35** (1987) 2697.
26. P. FELTHAM and N. KAUSER, *Phys. Status Solidi* (a) **117** (1990) 135.
27. M. Z. BUTT, *J. Phys.: Condens. Matter*, **2** (1990) 5797.
28. *Idem., Phil. Mag. Lett.* **60** (1989) 141.
29. *Idem., Solid State Commun.* **72** (1989) 139.
30. M. Z. BUTT, P. FELTHAM and I. M. GHAURI, *Phys. Status Solidi* (a) **80** (1983) K125.
31. *Idem., J. Mater. Sci.* **21** (1986) 2664.
32. M. Z. BUTT and P. FELTHAM, *Phys. Status Solidi* (a) **60** (1980) K167.
33. M. Z. BUTT, I. M. GHAURI, R. QAMAR, K. M. HASHMI and P. FELTHAM, *Acta Metall.* **29** (1981) 829.
34. M. Z. BUTT and M. A. KHAN, *Phys. Status Solidi* (a) **113** (1989) K189.
35. P. FELTHAM, *Phil. Mag.* A **49** (1984) 727.
36. *Idem., Phil. Mag.* A **57** (1988) 831.
37. *Idem., Phil. Mag.* B **57** (1988) 111.
38. M. Z. BUTT, K. M. CHAUDHARY and P. FELTHAM, *J. Mater. Sci. Lett.* **2** (1983) 713.
39. M. Z. BUTT and P. FELTHAM, *Metal Sci.* **18** (1984) 123.
40. M. Z. BUTT, K. M. HASHMI and P. FELTHAM, *J. Phys. F: Metal Phys.* **11** (1981) L275.
41. I. M. GHAURI, P. FELTHAM and M. Z. BUTT, *Phys. Status Solidi* (a) **96** (1986) K43.
42. P. FELTHAM, *Czech. J. Phys.* B **38** (1988) 519.
43. M. Z. BUTT and P. FELTHAM, *J. Mater. Sci.* **15** (1980) 253.
44. M. Z. BUTT, K. M. CHAUDHARY and P. FELTHAM, *J. Mater. Sci.* **18** (1983) 840.
45. *Idem., Fizika* **14** (1982) 163.
46. Z. S. BASINSKI, M. S. DUESBERY and G. S. MURTY, *Acta Metall.* **29** (1981) 801.
47. M. AHMAD, M. Z. BUTT, S. A. CHAUDHARY and I. M. GHAURI, *Phil. Mag.* A **54** (1986) L9.
48. P. FELTHAM, *Phys. Status Solidi* (b) **98** (1980) 301.
49. *Idem., Rev. Deform. Behav. Mater.* **4** (1982) 97.
50. M. Z. BUTT, M. I. NASIR and P. FELTHAM, *Res Mechanica Lett.* **1** (1981) 39.
51. P. FELTHAM, *Phys. Status Solidi* (a) **75** (1983) K95.
52. M. Z. BUTT, P. FELTHAM and S. M. RAZA, *Scripta Metall.* **17** (1983) 1337.
53. M. Z. BUTT and P. FELTHAM, *J. Mater. Sci. Lett.* **4** (1985) 302.
54. P. FELTHAM and M. Z. BUTT, *Crystal Res. & Technol.* **19** (1984) 325.
55. P. FELTHAM, *Scripta Metal.* **13** (1979) 119.
56. K. HASHIMOTO and H. MARGOLIN, *Acta Metall.* **31** (1983) 773, 787.
57. A. B. VOLYNTSEV, *Phys. Status Sol.* (b) **165** (1991) 343.
58. M. Z. BUTT, M. I. NASIR and R. QAMAR. *Fizika* **13** (1981) 365.
59. M. Z. BUTT and I. M. GHAURI, *Phys. Status Solidi* (a) **107** (1988) 187.
60. M. Z. BUTT, *J. Mater. Sci. Lett.* **7** (1988) 879.
61. M. Z. BUTT, S. A. CHAUDHARY and I. M. GHAURI, *Mater. Lett.* **7** (1989) 347.
62. M. Z. BUTT and M. A. SHAMI, *J. Mater. Sci.* **23** (1988) 2661.
63. M. Z. BUTT, *J. Mater. Sci. Lett.* **2** (1983) 1.
64. C. J. SPEARS and P. FELTHAM, *J. Phys.* (Paris) **44** (1983) CQ597.
65. P. LUKÁČ, Z. TROJANOVÁ and M. HAMERSKÝ, *Kovové Materiály* (Czech) **26** (1988) 96.
66. V. NAVRÁTIL, M. HAMERSKÝ, P. LUKÁČ, V. P. SOLDATOV and V. I. STARTSEV, *Phys. Status Solidi* (a) **75** (1983) K133.
67. M. Z. BUTT and A. SABOOH, to be published.
68. M. Z. BUTT and M. KALEEM, *Phys. Status Solidi* (a) **136** (1993) in press.
69. P. LUKÁČ and Z. TROJANOVÁ, *Phys. Status Solidi* (a) **53** (1979) K143.
70. M. Z. BUTT and M. NOSHI, to be published.
71. R. J. ARSENAULT and T. W. CADMAN, *Rev. Deform Behav. Mater.* **3** (1978) 5.
72. H. HENDERSON-BROWN and K. F. HALE, in "High-Voltage Electron Microscopy" (Academic Press, New York, 1976) p. 206.
73. B. M. STRUNIN, *Phys. Status Solidi* (a) **35** (1976) 551.
74. H. TRAUB, H. NEUHÄUSER and C. SCHWINK, *Acta Metall.* **25** (1977) 437.
75. *Idem., Acta Metall.* **25** (1977) 1289.
76. P. HAASEN, In "Dislocations in solids", Vol. 4, edited by F. R. N. Nabarro (North-Holland, Amsterdam, 1979) p. 155.
77. *Idem.*, in "Physical Metallurgy", 3rd Edn, Part II, edited by R. W. Cahn and P. Haasen (North-Holland, Amsterdam, 1983) p. 1341.
78. Z. S. BASINSKI, R. A. FOXALL and R. PASCUAL, *Scripta Metall.* **6** (1972) 807.
79. C. SCHWINK and T. WILLE, *Scripta Metall.* **14** (1980) 1093.
80. P. FELTHAM, *J. Phys. D: Appl. Phys.* **2** (1969) 377.
81. A. H. COTTRELL, "Dislocations and Plastic Flow in Crystals" (Clarendon Press, Oxford 1958) p. 142.
82. H. SAKA, *Phil. Mag.* A, **42** (1980) 185.
83. A. AKHTAR and E. TEGHTSOONIAN, *Acta Metall.* **17** (1969) 1339.

84. T. E. MITCHELL and P. R. THORNTON, *Phil. Mag.* **8** (1963) 1127.
85. V. P. PODKUYKO and V. V. PUSTOVALOV, *Cryogenics* **18** (1978) 589.
86. V. H. SCHARF, P. LUKÁČ, M. BOČEK and P. HAASEN, *Z. Metallk.* **59** (1968) 799.
87. S. TAKEUCHI, H. YOSHIDA and T. TAOKA, *Trans. Jap. Inst. Met.* **9** (1968) 715.
88. D. J. BACON and R. O. SCATTERGOOD, *Rev. Deform Behav. Mater.* **2** (1977) 317.
89. M. Z. BUTT, Z. RAFI and M. A. KHAN, *Phys. Status Solidi* (a) **120** (1990) K149.
90. M. Z. BUTT and Z. RAFI, *J. Mater. Sci. Lett.* **10** (1991) 309.
91. S. M. RAZA, *Scripta Metall.* **16** (1982) 1325.
92. S. NAKA and A. LASALMONIE, *Mater. Sci. Engng.* **56** (1982) 19.
93. *Idem.*, in "Titanium science and technology", edited by G. Lütjering, U. Zwicker and W. Bunk (Deutsche Ges. für Metallk., Stuttgart, 1985) p. 1797.
94. J. F. STOHR and J. P. POIRIER, *Phil. Mag.* **25** (1972) 1313.
95. R. C. BLISH and T. FREELAND Jr, *J. Appl. Phys.* **40** (1969) 884.
96. A. AKHTAR, *Scripta Metall.* **10** (1976) 365.
97. J. BEUERS, S. JONSSON and G. PETZOW, *Acta Metall.* **35** (1987) 2277.
98. M. Z. BUTT, PhD Thesis, Brunel University, London, UK (1978).
99. B. C. PETERS and A. A. HENDRICKSON, *Met. Trans.* **1** (1970) 2271.
100. C. D. STATHAM and J. W. CHRISTIAN, *Scripta Metall.* **5** (1971) 399.
101. F. FAUDOT and J. BIGOT, *J. Less-Common Met.* **56** (1971) 151.
102. M. ROJKO and P. LUKÁČ, *J. Mater. Sci.* **8** (1973) 1065.
103. P. LUKÁČ and I. STULÍKOVA, *Czech. J. Phys.* B **24** (1974) 648.
104. P. H. SCHARF, P. LUKÁČ, M. BOCĚK and P. HAASEN, *Z. Metallk.* **59** (1968) 799.
105. A. AKHTAR and E. TEGTHSOONIAN, *Acta Metall.* **17** (1969) 1339.
106. *Idem., Phil. Mag.* **25** (1972) 897.
107. A. URAKAMI, M. MESHII and M. E. FINE, in "Second International Conference on the strength of metals and alloys" (American Society for metals, California, 1970) p. 272.
108. W. F. SHEELEY, E. D. LEVINE and R. R. NASH, *Trans. Amer. Inst. Mech. Engng.* **215** (1959) 693.
109. K. KAMADA and I. YOSHIZAWA, *J. Phys. Soc. Japan*, **31** (1971) 1056.
110. R. H. HAMMAR, R. A. STRAHL and A. A. HENDRICKSON, *Trans. Japan Inst. Met.* **9** (1967) 708.
111. A. A. HENDRICKSON and M. E. FINE, *Trans. Amer. Inst. Mech. Engng.* **221** (1961) 967.
112. G. E. TARDIFF and A. A. HENDRICKSON, *ibid.*, **230** (1964) 586.
113. T. E. MITCHELL and P. L. RAFFO, *Canad. J. Phys.* **45** (1967) 1047.
114. B. C. PETERS and A. A. HENDRICKSON, *Met. Trans* **1** (1970) 2271.
115. P. HERKE, H. O. KIRCHNER and G. SCHOECK, in "Fourth international conference on the strength of metals and alloys" (American Society for Metals, Nancy, France, 1976). Vol. 1, p. 151.
116. T. SUZUKI, in "Second international conference on the strength of metals and alloys", Vol. 1 (American Society for Metals, Ohio, 1970) p. 237.
117. Z. S. BASINSKI, *Scripta Metall.* **8** (1974) 1301.
118. B. WIELKE, A. CHALUPKA, B. KAUFMANN, P. LUKÁČ and A. SVOBODOVA, *Z. Metallk.* **70** (1979) 85.
119. J. KRASOVA, P. KRATOCHVÍL and B. SMOLA, in "Fourth international conference on the strength of metals and alloys, Vol. 1 (American Society for Metals, Ohio, 1976) p. 256.
120. P. FELTHAM and N. KAUSER, *Phys. Status Solidi* (a) **133** (1992) 349.

Received 5 April
and accepted 7 August 1992